

Title Fukushima atmospheric dispersion
and dose assessment simulations
with ROSA and VALMA

Author(s) Ilvonen, Mikko; Takasuo, Eveliina;
Rossi, Jukka

Citation RESEARCH REPORT :
VTT-R-01377-13
VTT, 2013, pages 52.

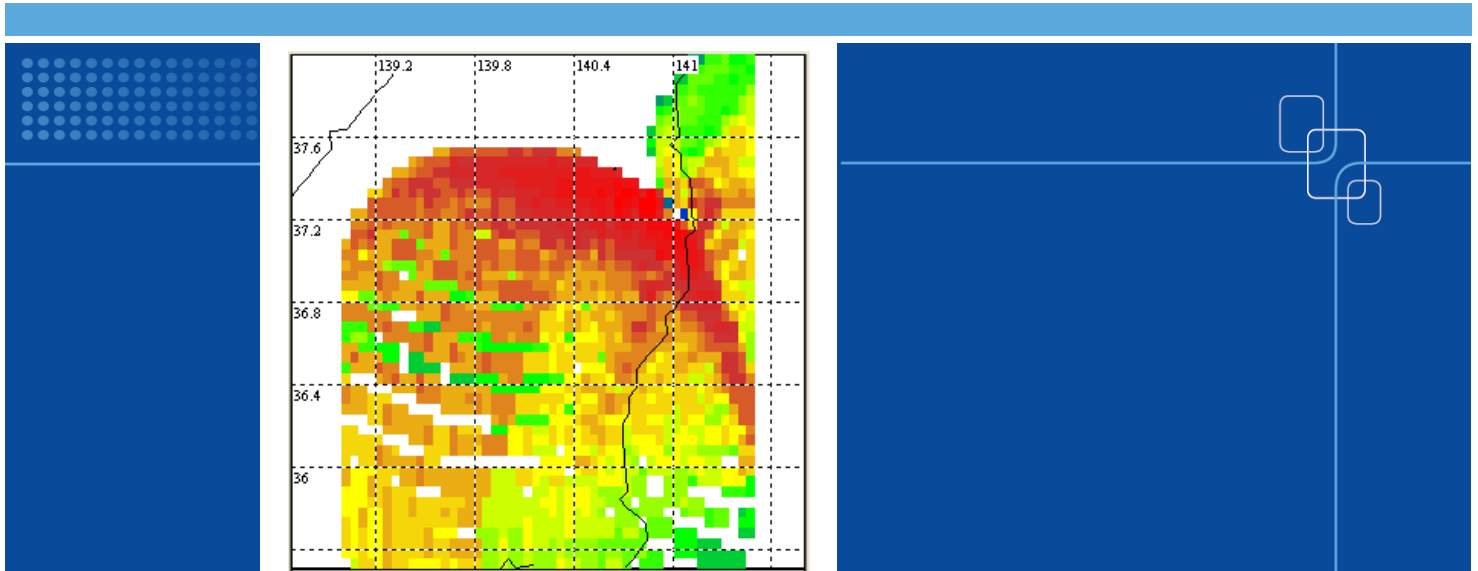
Rights This report may be downloaded for
personal use only.

VTT
<http://www.vtt.fi>
P.O. box 1000
FI-02044 VTT
Finland

By using VTT Digital Open Access Repository you are bound by the following Terms & Conditions.

I have read and I understand the following statement:


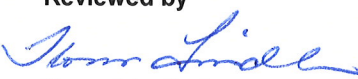
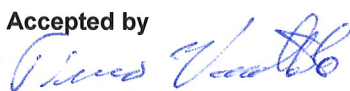

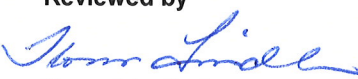
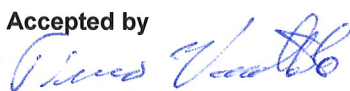

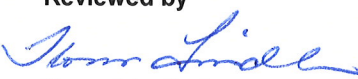
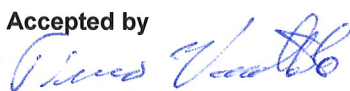
This document is protected by copyright and other intellectual property rights, and duplication or sale of all or part of any of this document is not permitted, except duplication for research use or educational purposes in electronic or print form. You must obtain permission for any other use. Electronic or print copies may not be offered for sale.



Fukushima atmospheric dispersion and dose assessment simulations with ROSA and VALMA

Authors: Mikko Ilvonen, Eveliina Takasuo, Jukka Rossi

Confidentiality: Public

| | | | | |
|---|---|---|---|--|
| Report's title Fukushima atmospheric dispersion and dose assessment simulations with ROSA and VALMA | | | | |
| Customer, contact person, address SAFIR2014 Finnish Research Programme on Nuclear Power Plant Safety | Order reference 3/2012SAF | | | |
| Project name Core debris coolability and environmental consequence assessment | Project number/Short name 77421/COOLOCE-E | | | |
| Author(s) Mikko Ilvonen, Jukka Rossi, Eveliina Takasuo | Pages 52 | | | |
| Keywords Fukushima, VALMA, source term, atmospheric dispersion, dose assessment, radiological consequences, deposition, external dose rate | Report identification code VTT-R-01377-13 | | | |
| Summary <p>Atmospheric dispersion simulations examining the nuclear power plant accident that occurred in Fukushima in March 2011 have been performed using two codes dedicated for estimating the consequences of accidental radioactive releases, ROSA and VALMA. A literature search was done to collect background material on source term estimates (including nuclide-specific released activities, temporal evolution and height distribution), measured fallout, concentration in air and external dose rates, as well as atmospheric dispersion simulations published by other authors. Scoping calculations of dose rates near the plant site were done with the ARANO-based ROSA code. VALMA inputs were prepared for a hypothetical weather mast at NPP site (data is actually interpolated from the ECMWF NWP model), for several source distribution assumptions, and for generating simulated results for some known measurement points. VALMA simulations were made and the results are available both on a map background (about 250 x 250 km around site) and as temporal trends at chosen geographical points. Comparisons of measurements and simulations have been made.</p> | | | | |
| Confidentiality | Public | | | |
| Espoo, 1.3.2013 <table border="0"> <tr> <td style="vertical-align: top;"> Written by  Mikko Ilvonen Principal Scientist, Team Leader </td> <td style="vertical-align: top; text-align: center;"> Reviewed by  Ilona Lindholm, Principal Scientist </td> <td style="vertical-align: top;"> Accepted by  Timo Vanttola Technology Manager </td> </tr> </table> | | Written by  Mikko Ilvonen Principal Scientist, Team Leader | Reviewed by  Ilona Lindholm, Principal Scientist | Accepted by  Timo Vanttola Technology Manager |
| Written by  Mikko Ilvonen Principal Scientist, Team Leader | Reviewed by  Ilona Lindholm, Principal Scientist | Accepted by  Timo Vanttola Technology Manager | | |
| VTT's contact address P.O. Box 1000, 02044 VTT, Finland | | | | |
| Distribution (customer and VTT) SAFIR2014 Reference Group 5 VTT: Kaisa Simola, Vesa Suolanen, Timo Vanttola, Tuomo Sevón | | | | |
| <p><i>The use of the name of the VTT Technical Research Centre of Finland (VTT) in advertising or publication in part of this report is only permissible with written authorisation from the VTT Technical Research Centre of Finland.</i></p> | | | | |

Contents

| | |
|--|----|
| Contents..... | 2 |
| 1. Introduction..... | 4 |
| 2. Dispersion and dose assessment in brief..... | 5 |
| 3. The Fukushima NPP accident in 2011 | 6 |
| 3.1 Atmospheric conditions..... | 7 |
| 4. Source term | 8 |
| 4.1 Temporal trends of releases | 11 |
| 4.2 Measurement data..... | 15 |
| 5. ROSA simulations..... | 26 |
| 5.1 Main features of the code | 26 |
| 5.2 Source term..... | 26 |
| 5.3 Atmospheric dispersion..... | 27 |
| 5.4 Exposure pathways | 27 |
| 5.5 Input | 28 |
| 5.6 Output..... | 28 |
| 5.7 Simulation of the Fukusima dose rates | 29 |
| 6. VALMA simulations..... | 30 |
| 6.1 Code description..... | 30 |
| 6.1.1 Input and other initialization | 31 |
| 6.1.2 Particle trajectories and calculation time steps..... | 31 |
| 6.1.3 Calculation of the result quantities of dose assessment..... | 32 |
| 6.1.4 Transformation into grid representation..... | 33 |
| 6.1.5 Use of weather data measured by mast equipment | 33 |
| 6.2 Input | 34 |
| 6.2.1 Weather data | 37 |
| 6.3 Results | 40 |
| 6.3.1 Particle trajectories | 40 |
| 6.3.2 Concentrations..... | 41 |
| 6.3.3 Depositions..... | 44 |
| 6.3.4 Dose rates | 45 |
| 7. Other simulations..... | 46 |
| 8. Discussion | 47 |
| 8.1 Concentrations..... | 48 |
| 8.2 Depositions..... | 48 |
| 8.3 Dose rates | 49 |
| 8.4 Suggestions for future work | 49 |
| 9. Conclusions | 50 |
| References..... | 51 |

1. Introduction

A magnitude 9 earthquake occurred near the Pacific coast of Honshu, Japan, on March 11, 2011, followed by a large tsunami that resulted in the loss of more than 20000 lives and extensive damage to buildings and infrastructure. One of the consequences was a station blackout at the Fukushima Dai-ichi nuclear power plant. The loss of power developed into a severe accident with core damage at several reactor units causing radioactive releases into the air and the ocean. The accident was categorized as a Class 7 accident on the International Nuclear and Radiological Event Scale (INES). Only Chernobyl has been previously rated into this class, however, it should be mentioned that the amount of radionuclides discharged into the environment was clearly smaller in the case of Fukushima due to a very different type of accident progression and plant design.

In this work, we have collected information of the accident source term (i.e. nuclide-wise radioactive atmospheric release as function of time and release height), radionuclide air concentrations and depositions and external radiation dose rates from public literature, and acquired meteorological data during the accident via the Finnish Meteorological Institute (FMI). Based on the collected information, atmospheric dispersion simulations have been run using two codes dedicated for estimating the consequences of radioactive releases, ROSA and VALMA. The results have been compared to the measurements of the dose rates, concentrations and deposited amounts of certain nuclides in the vicinity of the plant site, and to estimates given by other reported simulations. The objectives of the work were to assess the performance of the two codes used in Finland against a real and highly topical severe accident, and to introduce a new researcher into the topic.

ROSA and VALMA are based on the Lagrangian principles of dispersion modelling and calculate the trajectories of the pollutant particles in the atmosphere. ROSA is best suited for calculating short-range, short-duration releases, utilizing weather data for a given point (usually the weather mast of the NPP, through online connection). VALMA is a more advanced code that accounts for the meteorological conditions in a more detailed manner than ROSA, e.g. by replacing ROSA's linear central trajectories by freely winding ones. Both codes are used in Finland as a part of emergency preparedness for abnormal radiation situations: VALMA is used by STUK (Radiation and Nuclear Safety Authority) and ROSA by the utility company TVO.

The meteorological data obtained by the authors from FMI is based on the weather prediction model of European Centre on Medium-Range Weather Forecast (ECMWF). It consists of the wind speed, dispersion direction, precipitation rate, cloud coverage and stability class for the time interval of March 10 - May 9, 2011. The weather data is one-point data, interpolated from a numerical 3D weather prediction model, to the nuclear power plant site and presented at intervals of one hour.

The presented work has been financed by SAFIR2014, the Finnish research programme on nuclear power plant safety, as a subproject in the COOLOCE-E project in 2012. The topic of environmental consequence assessment continues to be important due to the topicality and on-going analyses of the Fukushima Dai-ichi accident. In addition, the training of new experts in this area has been noted necessary by the Finnish research community. It is expected that the work presented in this report will continue in the future.

2. Dispersion and dose assessment in brief

The main phenomena of atmospheric dispersion and dose assessment are presented in the following list, with a brief explanation of each term.

- Radioactive source term

The source term describes the amounts and types of radionuclides that have been released into the environment at the site of the emission, i.e. the source for the potential exposure to radioactivity. This includes the temporal and spatial (height) distributions of the different nuclides at the source. These are extremely important due to the change of weather conditions as a function of time and location.

- Atmospheric advection and dispersion

In meteorology, advection means the (horizontal) transport of some quantity by the “bulk flow” of air in the atmosphere. Advection describes how the radionuclides are carried by winds. Turbulent dispersion describes the mixing and entrainment of the emission particles with non-polluted air in the atmosphere by turbulent fluctuations. The amount of atmospheric turbulence has a significant effect on the air concentrations and spreading of the particles. Typically, the effect of turbulence is described (rather coarsely) by atmospheric stability classes (e.g. Pasquill-Gifford).

- Radioactive chain decay

The decay chains of the radionuclides emitted into the environment are taken into account in dispersion modeling because the duration of the emission is relatively long. The radiological consequences depend on which nuclides are present in the emission plume, at the passage of the pollutant cloud and at the time of deposition to the ground.

- Deposition (fallout)

Deposition means the descent of nuclides from the atmosphere to the earth’s surface which can be divided to dry and wet deposition. The former consists of the descent of heavier particles by gravitational sedimentation and adsorption of lighter “gas-like” particles to surfaces, the latter means the scavenging of particles by precipitation (rain, snow or fog). Both decrease the concentrations in air but increase the activity on ground surfaces.

- Radiation exposure pathways

The exposure pathways (the way in which the radiation dose enters the human body) can be divided to external and internal. External dose is caused by a source of radiation outside the body, e.g. the gamma radiation directly from the plume or deposited nuclides on ground surfaces. Internal dose is caused by a radioactive substance that has ended up inside the body by inhalation, ingestion (eating and drinking) or through the skin by absorption or through a wound.

- Adverse effects of exposure to ionizing radiation

Radiation exposure can cause adverse health effects to the population as well as contamination of large areas. Some of the health effects are stochastic and appear in long-term as the result of exposure to relatively low levels of radiation, such as the increased risk of cancer and genetic damage. Short-term exposure to high-level radiation leads to acute health effects, e.g. radiation sickness. In addition to the health effects to the individuals in the population, a radioactive emission can cause great economical losses. Contamination of soil in the path of the emission plume might leave large areas unavailable for agriculture and residential use, and restriction to food and water consumption may be imposed. The economical effects consist of the monetary value assigned to the health effects, land use restrictions and damage to property, and their complete evaluation is usually difficult.

- Radiological countermeasures

Countermeasures aim at avoiding the adverse effects of the radioactive discharge: Depending of the severeness of the accident, they include e.g. evacuation, sheltering inside buildings, taking potassium iodide tablets and protecting food supplies. The atmospheric dispersion models play an important role in determining the necessary countermeasures, they are used by licensees and authorities as a means to plan the response to radiation emergencies.

3. The Fukushima NPP accident in 2011

The Fukushima Dai-ichi nuclear power plant consists of six boiling water reactors designed by General Electric (GE) and operated by the Tokyo Electric Power Company (TEPCO). An overview of the Fukushima Dai-ichi reactor units and their operating status when the earthquake occurred are presented in Figure 1. Unit 4 had been de-fuelled and units 5-6 were in shutdown due to maintenance outage, units 1-3 were operating normally.

| | Unit 1 | Unit 2 | Unit 3 | Unit 4 | Unit 5 | Unit 6 |
|-----------------------------------|-----------|-----------|-----------|------------|------------|------------|
| Electric power output (MW) | 460 | 784 | 784 | 784 | 784 | 1100 |
| Begin commercial operation | 1971 | 1974 | 1976 | 1978 | 1978 | 1979 |
| Reactor model | BWR 3 | BWR 4 | BWR 4 | BWR 4 | BWR 5 | BWR 5 |
| Containment type | Mark-1 | Mark-1 | Mark-1 | Mark-1 | Mark-1 | Mark-2 |
| Operating/time of shut-down | operating | operating | operating | 2010-11-29 | 2011-01-02 | 2010-08-13 |
| Number of fuel assemblies in core | 400 | 548 | 548 | 0 | – | – |
| Number of fuel assemblies in pond | 392 | 615 | 566 | 1535 | 994 | 940 |

Figure 1. Overview of the Fukushima Dai-ichi NPP units and their status at the occurrence of the earthquake (Stohl et al. 2012).

The earthquake that triggered the tsunami occurred at 14:46 (05:46 UTC) on March 11 in 2011. At the same time, the plant units at Fukushima were automatically shut down. The first tsunami struck the plant site at 15:27, followed by a second tsunami with the estimated height of 14 m at about 15:46. The second tsunami flooded over the seawalls protecting the plant site and inundated the plant facilities, disabling the emergency diesel generators. After this, the removal of the decay heat relied on steam-powered pump systems: mainly the isolation condenser at unit 1 and the reactor and containment isolation cooling system (RCICS) at units 2-6.

When the off-site power was not restored, the remaining emergency cooling systems were ultimately not capable of maintaining the water level in the reactor cores, resulting in various degrees of core damage and melting in units 1-3. The first emissions to the environment were reported at about 10:09 on March 12 due to venting of steam from unit 1 to lower the containment pressure. (The exact time of the start of the release is not known.) A hydrogen explosion which destroyed the roof of the reactor building occurred at unit 1 later on March 12, at 15:36, leaving the spent fuel pool in the upper part of the building exposed to atmosphere.

Further containment venting was done at units 1 and 3 on March 13. A second hydrogen explosion damaged the reactor building of unit 3 on March 14 at 11:01 and a third was suspected to have caused some damage within the unit 2 reactor building on March 15, with damage to the suppression chamber (wetwell) of the primary containment. The last of the hydrogen explosions occurred on March 15 at unit 4, causing damage to the upper part of the reactor building which had already been damaged in a fire on the same day.

The conditions and possible boiling in the spent fuel pools located in the upper part of the reactor buildings was a significant concern during March 15-20, and tonnes of seawater were injected into the pools of units 1-4 to control their temperature. The efforts were made more difficult by high levels of radiation (400 mSv/h) measured in the vicinity on unit 3 on March 15, the source of which was suspected to be the loss of coolant in the unit's spent fuel pool. Offsite electrical power became available to the six plant units on March 21-22. However, repairs and check-ups of the electrical equipment affected by the tsunami had to be performed before the external power could be restored.

The radionuclide emissions from the damaged reactor units reached their peak during 15-16 March as a result of the containment ventings and hydrogen explosions. After March 16 the release rate declined steadily. During the first weeks, I-131 was the main contributor to the doses. Later, the role of Cs-137 became more important as the half-life of I-131 is only about 8 days.

3.1 Atmospheric conditions

An approximate timeline of the atmospheric dispersion conditions during the accident is presented below. The timeline is based on information provided by FMI at the time the accident was on-going.

- Earthquake and tsunami on Friday, March 11, 2011, 05:46 UTC (14:46 local time)
-
- Emissions to the environment started on Saturday, March 12 (exact time not known)
- Until Monday, March 14: Spread direction was mainly towards sea.
 - Spread direction turned towards south, but winds were weak.
- Tuesday, March 15: Spread direction turns back to east / south-east, towards sea.
- Sunday, March 20: Cloudy, but no rain; winds rather weak, varying direction
- Monday, March 21: Low pressure heads to the east on the south side of Japan
 - Dispersion direction turns more to the west, meaning contamination of land areas; at the same time, wind speeds increase.

- Wind direction means the direction where air comes from (e.g. northerly wind: from north to south)
- Spread direction or dispersion direction: Direction to which pollutants are transported by wind
- On the northern hemisphere
 - Around a low pressure, winds circulate counter-clockwise
 - Around a high pressure, winds circulate clockwise
 - Wind speeds are highest near the center of low pressure
- Dry weather is over: Rains are approaching from west.
- Monday...Tuesday, March 21...22: 10 - 30 mm of rain was predicted.
- Wet deposition caused by rain is harmful for the rainy area.
- On the other hand, the radioactive cloud will be scavenged of nuclides and will be less harmful to the areas where it is transported.

4. Source term

The fission product inventory in the Fukushima reactors at the onset of the accident has been estimated by Ducros et al. (2012) whose estimate obtained by using the CESAR code is presented in Table 1. The same authors provide an estimate of the fraction of nuclides released to the environment (Table 2) and an analysis of release fraction of each nuclide against measured particle samples (Table 3). The release fractions according to nuclide class as given by a MELCOR model of Fukushima unit 1 are shown in Table 4 (Sevón, 2012). The reactor unit specific inventories of Xe-133 and Cs-137 as well as estimates of those in the spent fuel pools have been given by Stohl et al. (2012), shown in Table 5.

Table 1. Fission product core inventory at the time of reactor shutdown (Ducros et al. 2012).

| FP | CESAR activity (Bq/t _{HM}) | Total inventory of the 3 cores (Bq) |
|--------|--------------------------------------|-------------------------------------|
| Kr85 | 2.78E+14 | 7.29E+16 |
| Rb86 | 3.51E+13 | 9.20E+15 |
| Sr89 | 2.39E+16 | 6.25E+18 |
| Sr90 | 2.09E+15 | 5.48E+17 |
| Nb95 | 4.15E+16 | 1.09E+19 |
| Mo99 | 4.43E+16 | 1.16E+19 |
| Ru103 | 3.51E+16 | 9.21E+18 |
| Ru106 | 1.11E+16 | 2.90E+18 |
| Ag110m | 4.78E+13 | 1.25E+16 |
| Sb125 | 1.98E+14 | 5.19E+16 |
| Te127m | 3.11E+14 | 8.15E+16 |
| Te129m | 2.36E+15 | 6.19E+17 |
| Te132 | 3.34E+16 | 8.74E+18 |
| I131 | 2.34E+16 | 6.12E+18 |
| Xe133 | 4.86E+16 | 1.27E+19 |
| Cs134 | 2.78E+15 | 7.27E+17 |
| Cs136 | 9.19E+14 | 2.41E+17 |
| Cs137 | 2.77E+15 | 7.26E+17 |
| Ba140 | 4.25E+16 | 1.11E+19 |
| Ce144 | 3.21E+16 | 8.41E+18 |
| Eu154 | 1.21E+14 | 3.16E+16 |

Table II. FP core inventory at the reactor shut down (March 11, 2011)

Table 2. Activities released into the atmosphere from CEA and IRSN evaluations (Ducros et al. 2012)

| | Total FP released in the atmosphere (Bq) | FP inventory (CESAR calculation for the sum of the three cores) | Released Fraction (normalized to the 3 cores) | Unit 2 Released Fraction (Hyp 60% of the release coming from this unit) |
|----------------------------|--|---|---|---|
| Volatile FP | | | | |
| Cs137 (CEA ATM simulation) | 1.00E+16 | 7.26E+17 | 1.4% | 2.3% |
| I131 (CEA ATM simulation) | 4.00E+17 | 4.73E+18 | 8.5% | 14.0% |
| Cs134 | 2.78E+16 | 7.26E+17 | 3.8% | 6.3% |
| Cs137 | 2.06E+16 | 7.26E+17 | 2.8% | 4.7% |
| I131 | 1.97E+17 | 4.73E+18 | 4.2% | 6.9% |
| I133 | 4.20E+16 | 1.16E+18 | 3.6% | 6.0% |
| Te132 | 1.08E+17 | 4.57E+18 | 2.4% | 3.9% |
| Te129m | 1.22E+16 | 5.82E+17 | 2.1% | 3.5% |
| Semi-volatile FP | | | | |
| Ba140 | 1.12E+15 | 9.45E+18 | 1.18E-04 | 1.96E-04 |
| Low volatile FP | | | | |
| Nb95 | 1.08E+13 | 1.09E+19 | 9.95E-07 | 1.65E-06 |
| Sr89 | 4.33E+13 | 6.00E+18 | 7.22E-06 | 1.19E-05 |
| Sr90 | 3.27E+12 | 5.48E+17 | 5.97E-06 | 9.87E-06 |

Table 3. Analysis of an air particulate sample collected on March 22, 2011 at Takasaki (Ducros et al. 2012). Fr is 'normalized release fraction' of the nuclide Rn according to the following formula of Ducros et al: $Fr = (Rn/Rn_0) / ({}^{137}Cs/{}^{137}Cs_0)$; each of the two ratios means measured activity divided by calculated core inventory.

| Radionuclide | Type | Core inventory calculation (TBq/tM) | Measured activity concentration (Bq/m3) | Fr |
|--------------|---------------|-------------------------------------|---|----------|
| Rb86 | Volatile | 2.42E+01 | 2.83E-04 | 9.13E-01 |
| Nb95 | Low volatile | 4.11E+04 | 2.88E-04 | 5.49E-04 |
| Mo99 | Semi-volatile | 3.55E+03 | 4.11E-03 | 9.06E-02 |
| Ru103 | Low volatile | 2.95E+04 | 4.95E-05 | 1.32E-04 |
| Ag110m | Volatile | 4.65E+01 | 6.55E-05 | 1.10E-01 |
| Sb125 | Volatile | 1.98E+02 | 3.21E-04 | 1.27E-01 |
| Te127m | Volatile | 3.01E+02 | 6.03E-03 | 1.57E+00 |
| Te129 | Volatile | 1.92E+03 | 3.47E-02 | 1.41E+00 |
| Te129m | Volatile | 1.92E+03 | 5.49E-02 | 2.23E+00 |
| Te132 | Volatile | 3.21E+03 | 1.00E-01 | 2.44E+00 |
| I131 | Volatile | 9.87E+03 | 2.18E+00 | 1.73E+01 |
| Cs134 | Volatile | 2.75E+03 | 3.63E-02 | 1.03E+00 |
| Cs136 | Volatile | 5.40E+02 | 5.54E-03 | 8.04E-01 |
| Cs137 | Volatile | 2.77E+03 | 3.54E-02 | 1.00E+00 |
| Ba140 | Semi-volatile | 2.47E+04 | 2.87E-04 | 9.10E-04 |

Table 4. Radionuclides released to the environment in 50 hours, MELCOR simulation by Sevón (2012).

| Class name | Most important elements | Release (fraction of core inventory) | |
|---------------------------------|-------------------------|--------------------------------------|---------------------|
| Noble gases | Xe, Kr | 4E-1 | |
| Alkali metals | Cs, Rb | 3E-4 | Including Cs in CsI |
| Alkaline earths | Ba, Sr | 2E-6 | |
| Halogens | I, Br | 4E-4 | Including I in CsI |
| Chalcogens | Te, Se | 2E-4 | |
| Platinoids | Ru, Pd, Rh | 4E-8 | |
| Transition metals | Mo, Tc, Nb | 4E-4 | |
| Tetravalents | Ce, Zr, Np, Pu | 4E-8 | |
| Trivalentes | La, Pm, Y, Pr, Nd | 8E-9 | |
| Uranium | U | 5E-7 | |
| More volatile main group metals | Cd, As, Sb | 7E-4 | |
| Less volatile main group metals | Ag, Sn | 6E-4 | |

Table 5. Estimated inventories of radionuclide sources in Fukushima units 1-4 (Stohl et al. 2012).

| Source | ^{133}Xe (Bq) | ^{137}Cs (Bq) |
|-------------------------|------------------------|------------------------|
| Core unit 1 | 2.72×10^{18} | 2.40×10^{17} |
| Core unit 2 | 4.85×10^{18} | 2.59×10^{17} |
| Core unit 3 | 4.85×10^{18} | 2.59×10^{17} |
| Total cores | 1.24×10^{19} | 7.58×10^{17} |
| SFP unit 1 | 1.50×10^{12} | 2.21×10^{17} |
| SFP unit 2 | 2.59×10^{12} | 4.49×10^{17} |
| SFP unit 3 | 2.59×10^{12} | 3.96×10^{17} |
| SFP unit 4 | 1.04×10^{13} | 1.11×10^{18} |
| Total SFPs | 1.71×10^{13} | 2.18×10^{18} |
| Grand total | 1.24×10^{19} | 2.94×10^{18} |
| Total cores/grand total | 1.0 | 0.258 |

4.1 Temporal trends of releases

The timescale of the radionuclide releases have been estimated by several authors. The (preliminary) estimated temporal variation of I-131 and Cs-137 release rates reported by Chino et al. (2011) are presented in Figure 2 and Table 6. The release rates according to Nagai et al. (2012) are presented in Figure 3.

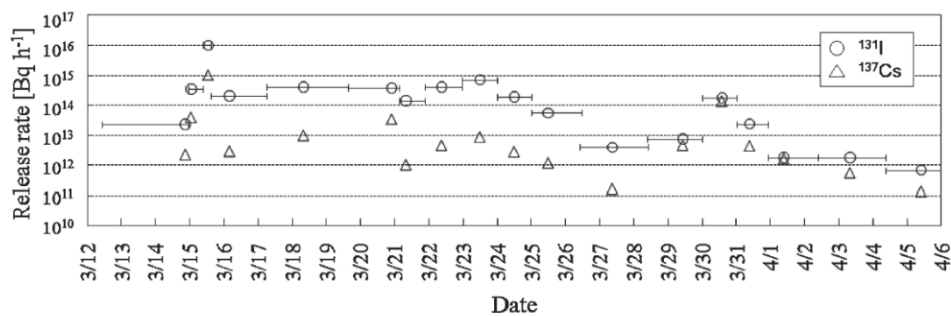


Figure 2. Release rates of I-131 and Cs-137 during March 12 – April 6, 2011. Lateral bars show the estimated release durations of I-131 (Chino et al. 2011).

Table 6. Release rates of I-131, radioactivity ratio of I-131/Cs-137 and duration times (Chino et al. 2011).

Table 2 Preliminary estimated release rates of ¹³¹I, radioactivity ratio of ¹³¹I/¹³⁷Cs, and duration times

| Dust sampling data No. | [Bq m ⁻³] | Calculations [Bq m ⁻³] | Release rate [Bq h ⁻¹] | ¹³¹ I/ ¹³⁷ Cs | Released time of sampled air | Duration |
|------------------------|------------------------------|------------------------------------|------------------------------------|-------------------------------------|------------------------------|--------------------|
| 1 | 6.8 | 3.0 × 10 ⁻¹³ | 2.3 × 10 ¹³ | 10 | 3/14 21:00 | 3/12 10 to 3/14 23 |
| 2 | 2,800 | 8.0 × 10 ⁻¹² | 3.5 × 10 ¹⁴ | 8.8 | 3/15 1:00 | 3/14 23 to 3/15 09 |
| — | Estimated from air dose rate | | 1.0 × 10 ¹⁶ | 10 | 3/15 13:00 | 3/15 09 to 3/15 15 |
| 3 | 830 | 4.0 × 10 ⁻¹² | 2.1 × 10 ¹⁴ | 70 | 3/16 4:00 | 3/15 15 to 3/17 06 |
| 4 | 33 | 8.0 × 10 ⁻¹⁴ | 4.1 × 10 ¹⁴ | 41 ^{b)} | 3/18 8:00 | 3/17 06 to 3/19 15 |
| 5 | 1,900 | 5.0 × 10 ⁻¹² | 3.8 × 10 ¹⁴ | 11 | 3/20 22:00 | 3/19 15 to 3/21 03 |
| 6 | 1,420 | 1.0 × 10 ⁻¹¹ | 1.4 × 10 ¹⁴ | 131 ^{c)} | 3/21 8:00 | 3/21 03 to 3/21 21 |
| 7 | 410 | 1.0 × 10 ⁻¹² | 4.1 × 10 ¹⁴ | 87 ^{c)} | 3/22 9:00 | 3/21 21 to 3/22 23 |
| 8 | 355 ^{a)} | 5.0 × 10 ⁻¹³ | 7.1 × 10 ¹⁴ | 80 | 3/23 12:00 | 3/22 23 to 3/24 00 |
| 9 | 193 | 1.0 × 10 ⁻¹² | 1.9 × 10 ¹⁴ | 66 | 3/24 12:00 | 3/24 00 to 3/25 00 |
| 10 | 555 | 1.0 × 10 ⁻¹¹ | 5.6 × 10 ¹³ | 45 | 3/25 12:00 | 3/25 00 to 3/26 11 |
| 11 | 20 | 5.0 × 10 ⁻¹² | 4.0 × 10 ¹² | 23 | 3/27 9:00 | 3/26 11 to 3/28 10 |
| 12 | 75 | 1.0 × 10 ⁻¹¹ | 7.5 × 10 ¹² | 1.6 | 3/29 10:30 | 3/28 10 to 3/30 00 |
| 13 | 180 | 1.0 × 10 ⁻¹² | 1.8 × 10 ¹⁴ | 1.3 | 3/30 14:00 | 3/30 00 to 3/31 00 |
| 14 | 24 | 1.0 × 10 ⁻¹² | 2.4 × 10 ¹³ | 5.3 | 3/31 9:30 | 3/31 00 to 3/31 22 |
| 15 | 1.78 | 1.0 × 10 ⁻¹² | 1.8 × 10 ¹² | 1.1 | 4/1 9:30 | 3/31 22 to 4/02 09 |
| 16 | 8.84 | 5.0 × 10 ⁻¹² | 1.8 × 10 ¹² | 3.1 | 4/3 8:00 | 4/02 09 to 4/04 09 |
| 17 | 6.99 | 1.0 × 10 ⁻¹¹ | 7.0 × 10 ¹¹ | 4.9 | 4/5 10:00 | 4/04 09 to 4/06 00 |

^{a)}Two hourly data, 530 and 180 Bq m⁻³, were averaged.
^{b)}Interpolated from the ratios of Nos. 3 and 5 because only ¹³¹I was measured.
^{c)}Applied the ¹³¹I/¹³⁷Cs ratio measured at other points because only ¹³¹I was measured.

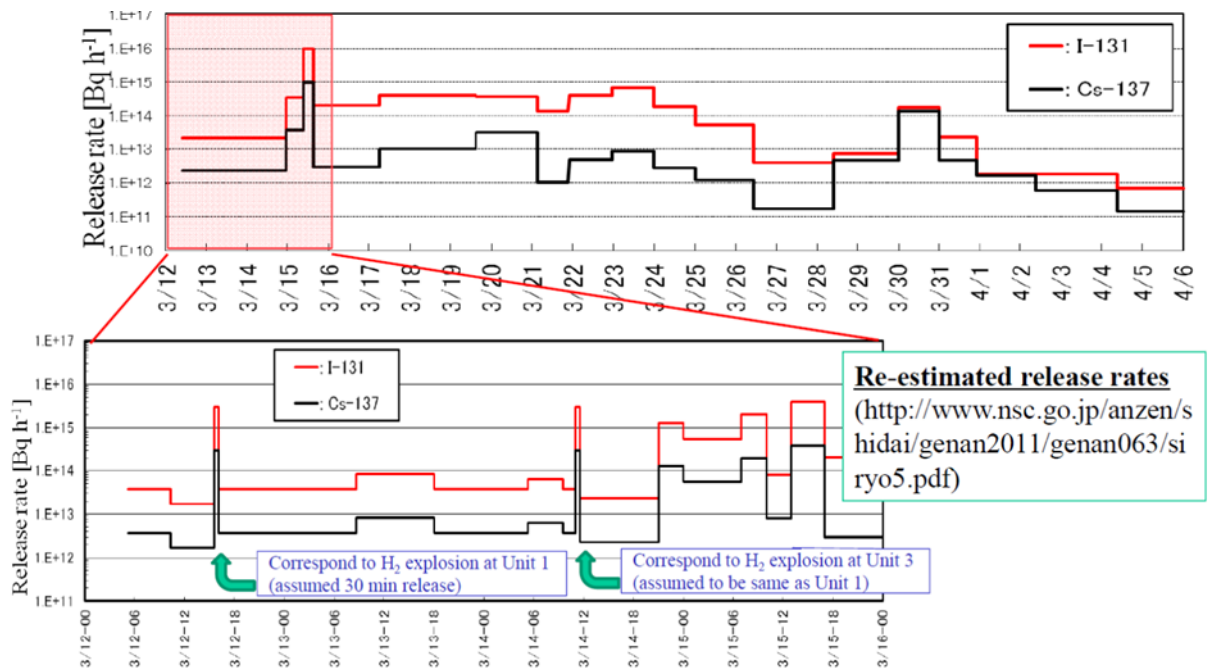


Figure 3. The release rates of I-131 and Cs-137 March 12 – April 6, 2011 (Nagai et al. 2012).

Stohl et al. (2012) have presented results of the Xe-133 and Cs-137 emissions. They provide a priori (first guess) estimates of the releases using available measurement data, and use a method of “inverse” modelling by an atmospheric transport model called FLEXPART to produce a more accurate, a posteriori estimation of the source term. The results of these analyses are shown in Figure 4 - Figure 7. Note that in each Figure, the curves represent temporal trends of release rate, whereas the background colours (yellow, turquoise, red) in Figures 6 – 7 represent the release height distribution (starting height of atmospheric transport).

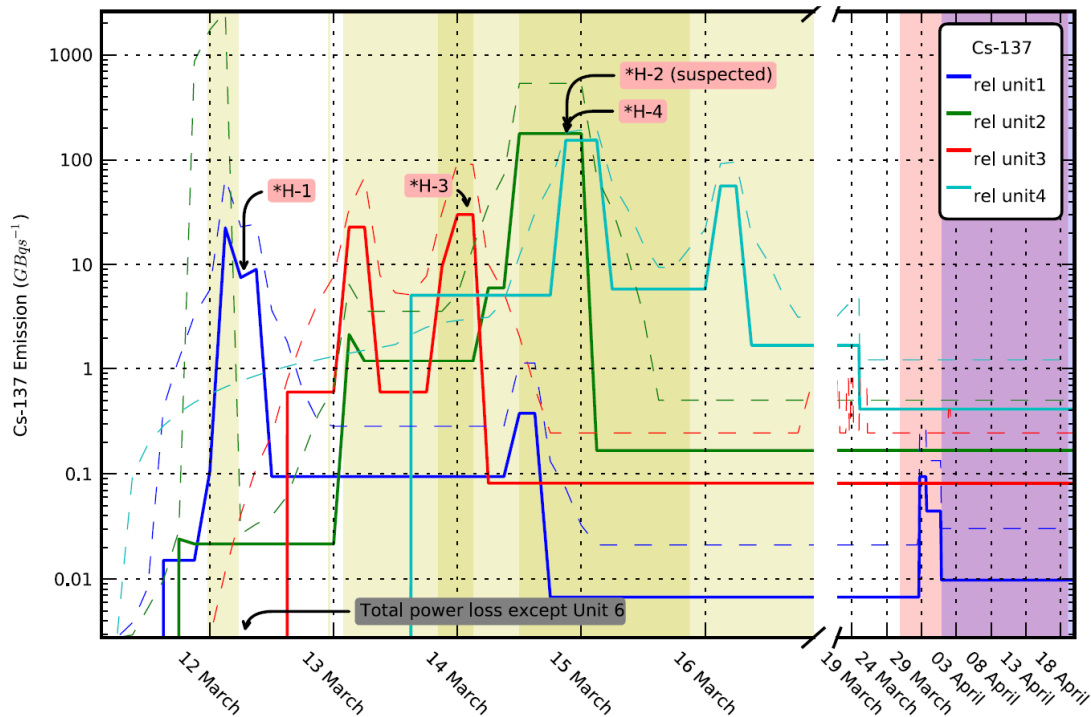


Figure 4. First guess emissions as a function of time for the four different reactor units for Cs-137. Emissions are drawn with coloured solid bold lines (blue, unit 1; green, unit 2; red, unit 3; sky blue, unit 4) and emission uncertainties with correspondingly coloured thin dashed lines (Stohl at al. 2012)

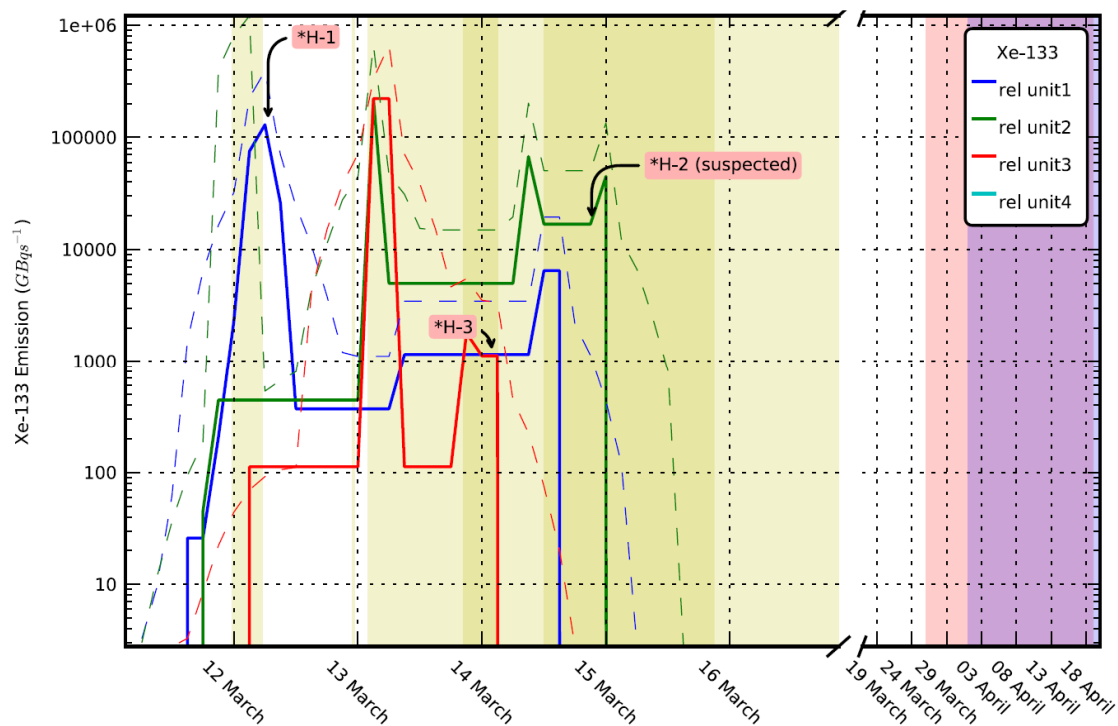


Figure 5. First guess emissions as a function of time for the four different reactor units for Xe-133. Emissions are drawn with coloured solid bold lines (blue, unit 1; green, unit 2; red, unit 3; sky blue, unit 4) and emission uncertainties with correspondingly coloured thin dashed lines (Stohl at al. 2012).

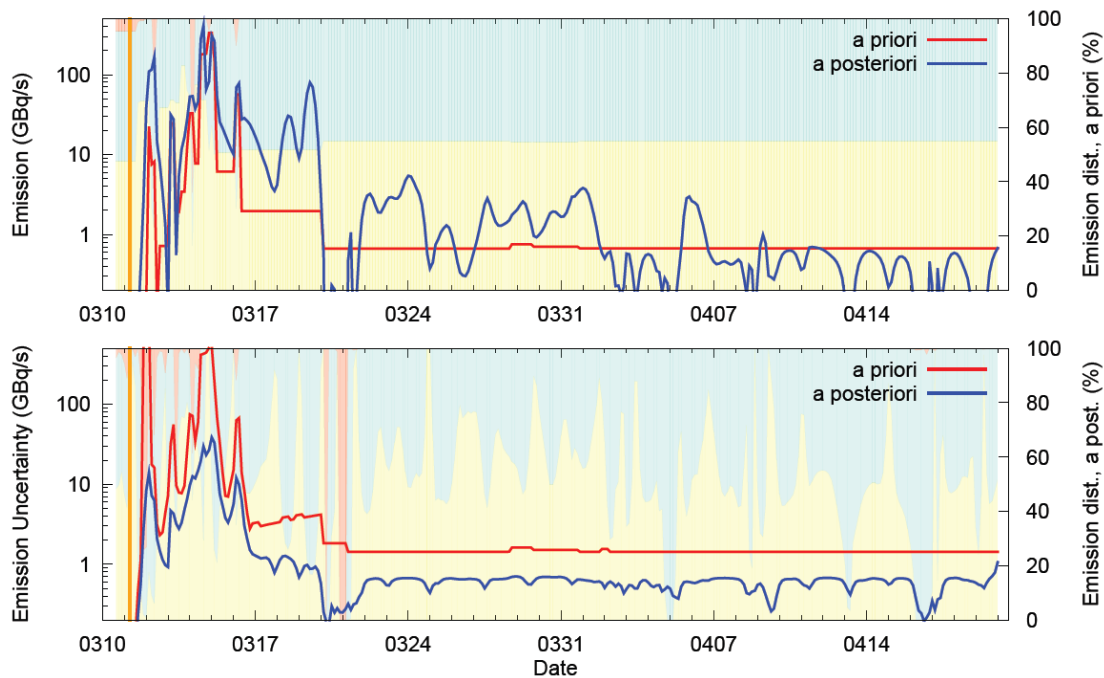


Figure 6. Emissions of Cs-137 used a priori (red line) and obtained a posteriori by the inversion (blue line) (upper panel), as well as associated uncertainties (lower panel). The vertical distribution of the emissions over the three layers, with scale on the right hand side, is shown by the background colors (0–50 m, light yellow; 50–300 m; light turquoise, 300–1000 m, light red) for the a priori emissions (upper panel) and the a posteriori emissions (lower panel). The orange vertical line indicates the time of the earthquake (Stohl et al. 2012).

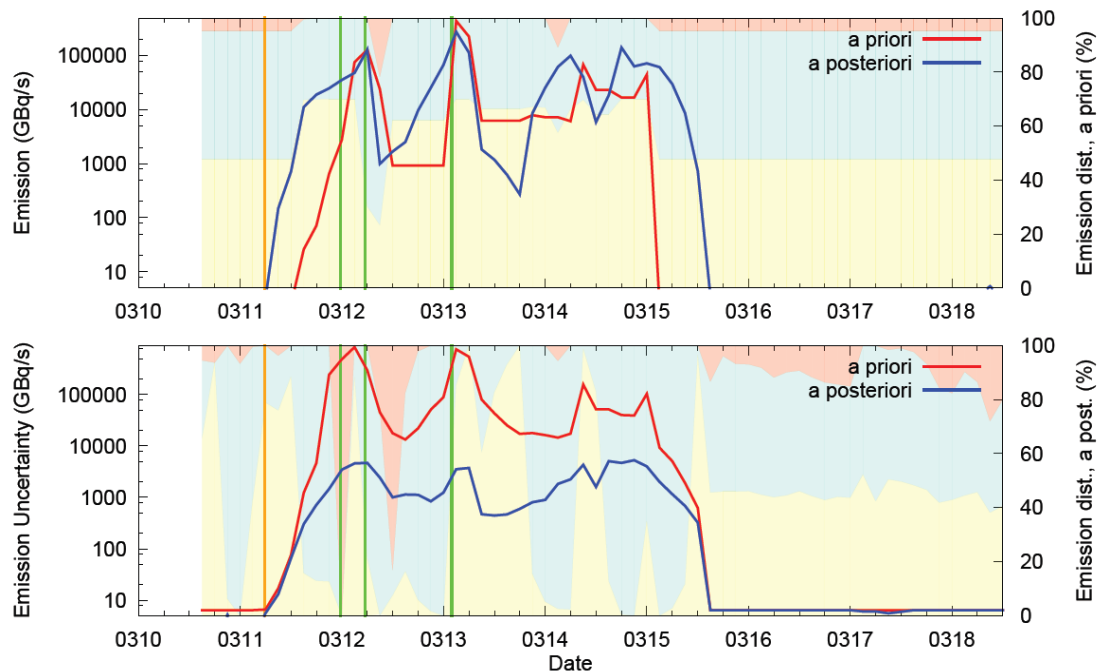


Figure 7. Emissions of Xe-133 used a priori (red line) and obtained a posteriori by the inversion (blue line) (upper panel), as well as associated uncertainties (lower panel). The vertical distribution of the emissions over the three layers, with scale on the right hand side, is shown by the background colors (0–50 m, light yellow; 50–300 m; light turquoise, 300–1000 m, light red) for the a priori emissions (upper panel) and the a posteriori emissions (lower panel). The orange vertical line indicates the time of the earthquake, and the green vertical lines mark the times when the first venting operations are reported (Stohl et al. 2012).

4.2 Measurement data

Measurement data of the radionuclide air concentrations, fallout and dose rates from different monitoring stations and samples have been reported by several authors. The comparisons of observed and simulated Cs-137 concentrations in Tokai-mura, Japan, by Stohl et al. (2012) are shown in Figure 8. An estimate of the monthly Cs-137 deposition in different locations in Japan is given by Hirose (2012) whose results are shown in Figure 9. I-131 concentrations during March 13 – 17 according to an estimate by Chino et al. (2011) are presented in Figure 10 (along with a simulation by SPEEDI dispersion model).

Radiation dose rates near Fukushima Dai-ichi have been reported by MEXT (the Japanese Ministry of Education, Culture, Sports, Science and Technology) and Hosoda et al. (2012) based on monitoring points in Japan. Examples of the dose rate data are shown in Figure 11 – Figure 13. The data reported by Hosoda et al. (2012) is based on car surveys conducted in March and April 2011. MEXT and the U.S. Department of Energy (2011) have performed measurements of dose rates and surface deposition of Cs within 80 km radius of Fukushima Dai-ichi. Their results are shown in Figure 14 and Figure 15.

Nagai et al. (2012) have presented monitoring data of air concentrations, Cs-137 depositions and dose rates in connection with simulations by the SPEEDI dispersion modelling package. Some of their results are presented in Figure 20 - Figure 23. The monitoring results that were found to be the most useful in the comparison to VALMA simulations are summarized at the end of the report in Table 9.

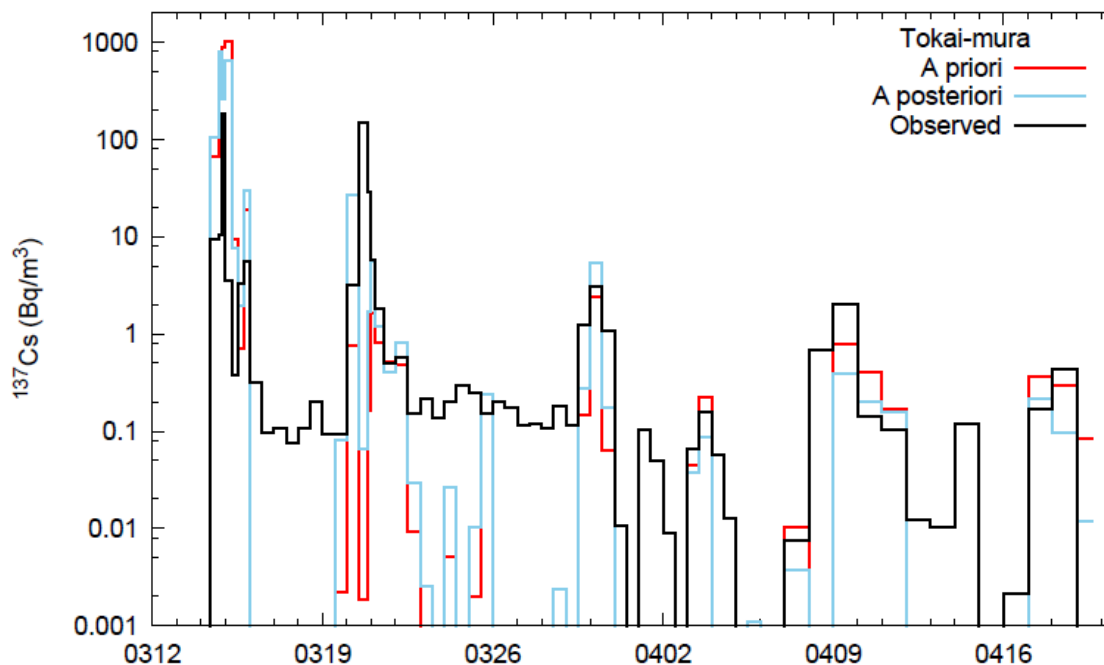


Figure 8. Time series of observed and simulated Cs-137 concentrations, based on a priori and a posteriori emissions for the station of Tokai-mura (Stohl et al. 2012). For the purposes of this study, the most important data is the black (observed) curve, which can be used to assess the corresponding result from VALMA simulations.

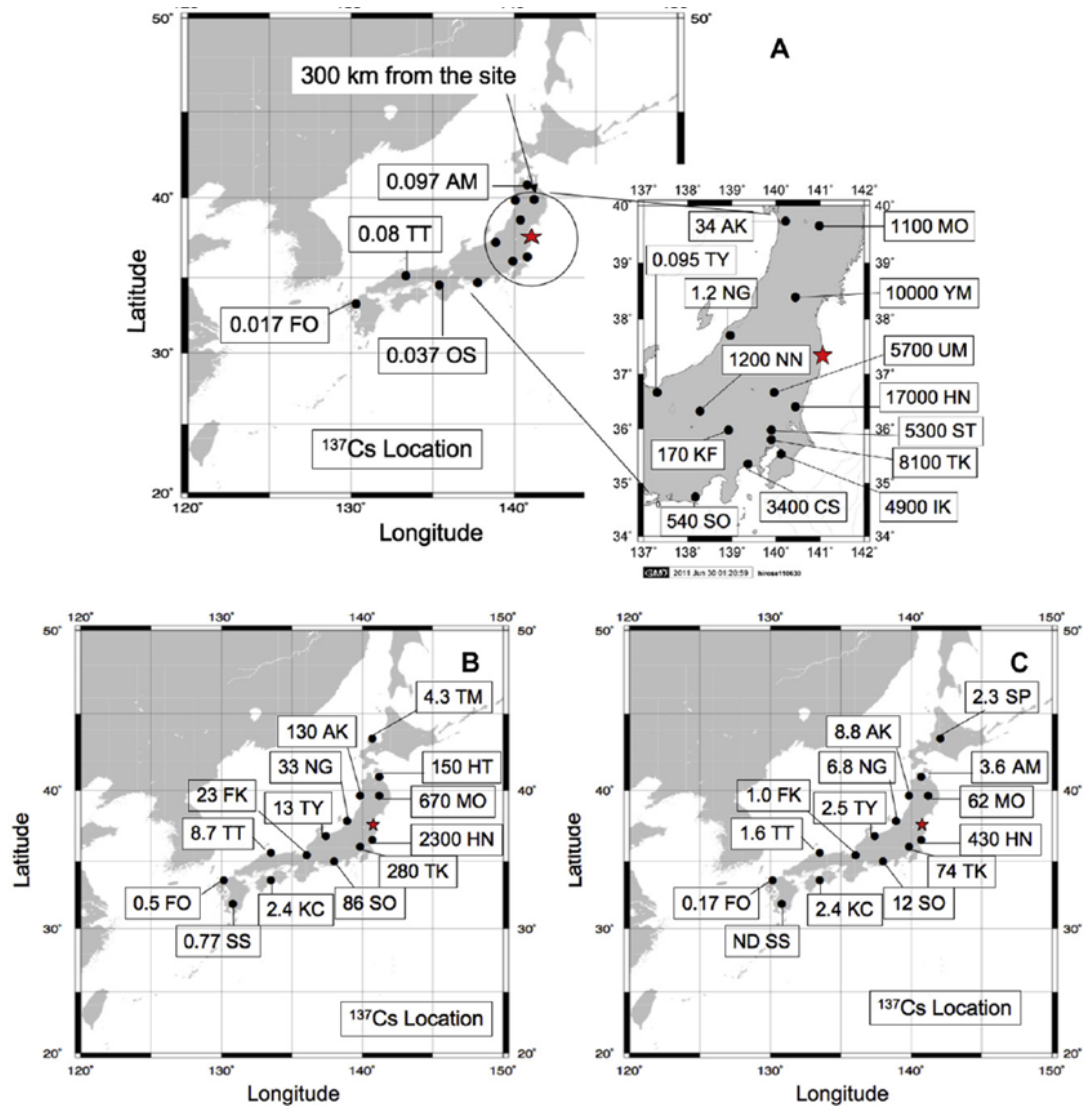


Figure 9. Spatial distributions of monthly Cs-137 deposition observed in Japan (Bq/m^2). A: March, B: April, C: May. AK: Akita, NI: Niigata, TY: Toyama, FK: Fukui, TT: Tottori, AM: Aomori, YM: Yamagata, MO: Morioka, UM: Utsunomiya, HN: Hitacihnaka, ST: Saitama, TK: Tokyo, KF: Kofu, IK: Ichihara, CS: Chigasaki, SO: Shizuoka, NN: Nagano, FO: Fukuoka, KC: Kochi, OS: Osaka, TM: Iwanai, HT: Higashi-Dori, SS: Satsuma-Sendai, SP: Sapporo (Hirose, 2012).

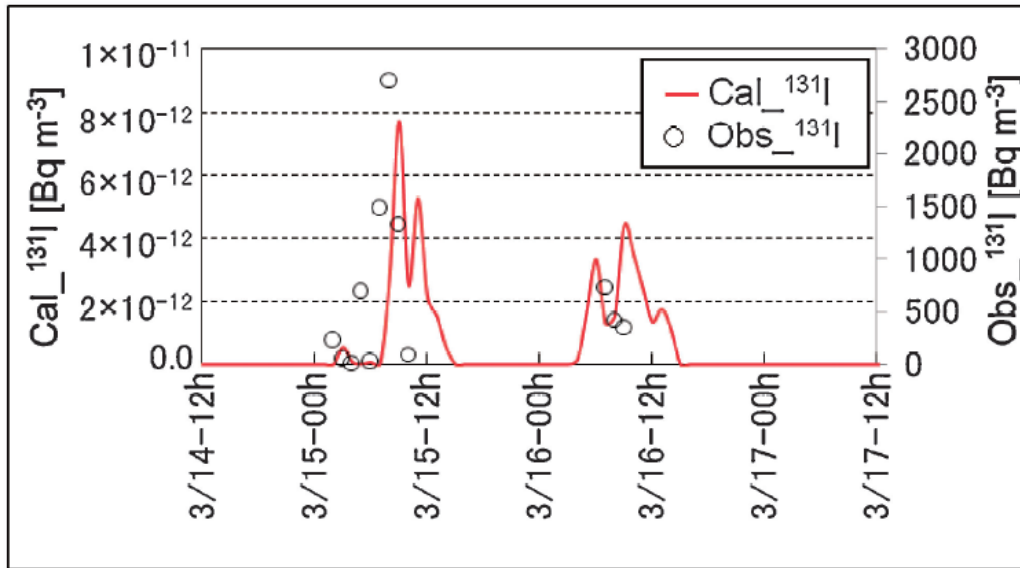


Figure 10. Comparison of temporal variation of air concentration of I-131 between measurement and calculation at JAEA, Tokai-mura, JST time (Chino et al. 2011).

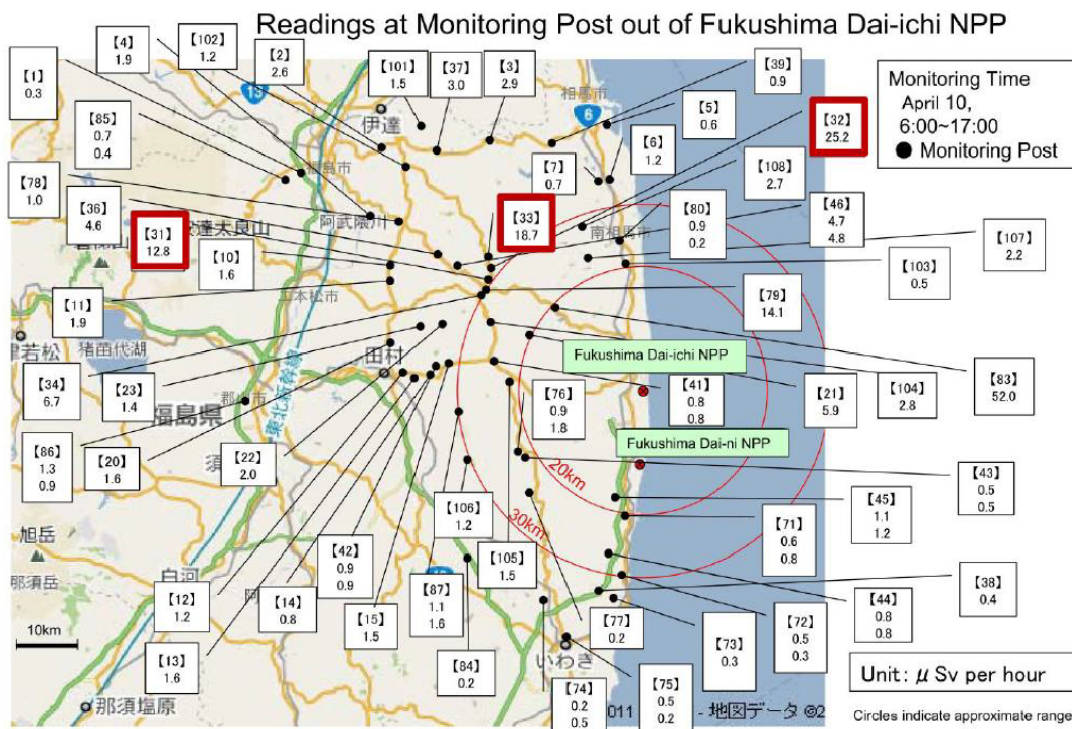


Figure 11. Dose rates at monitoring posts around Fukushima on April 10, 2011 (MEXT, 2013).

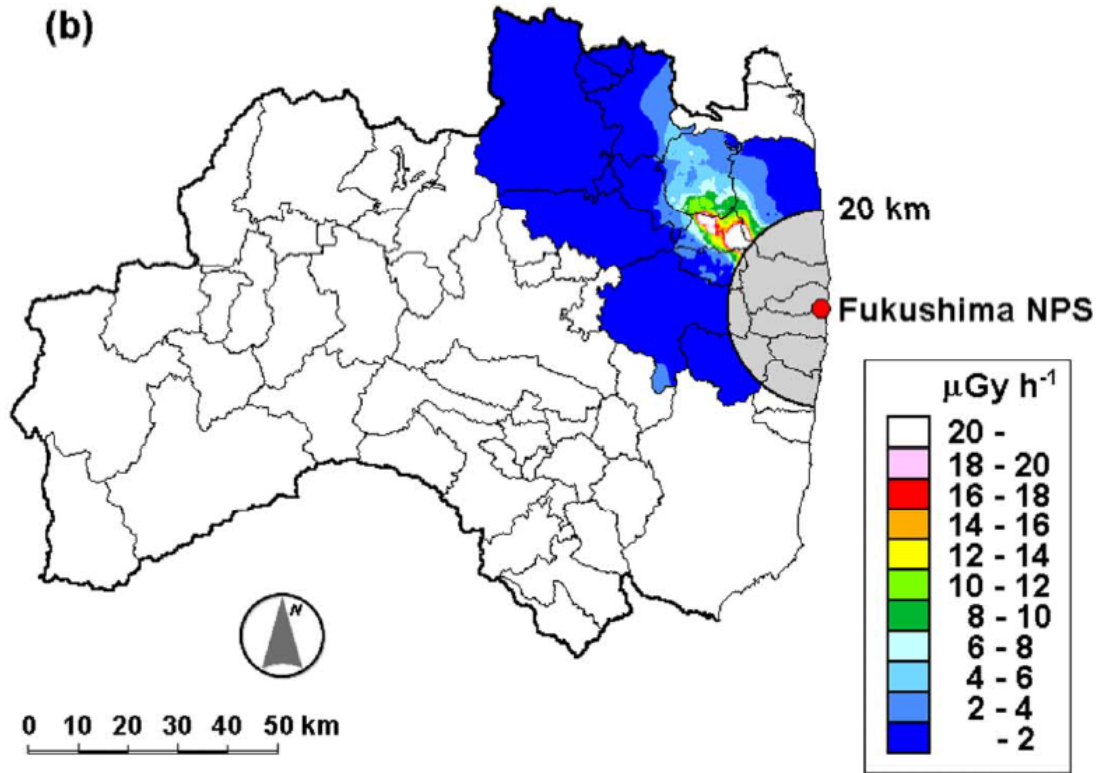


Figure 12. Distribution of the dose rates in air within the high level contamination area in Fukushima Prefecture. The rates were classified into eleven groups (Hosoda et al. 2012).

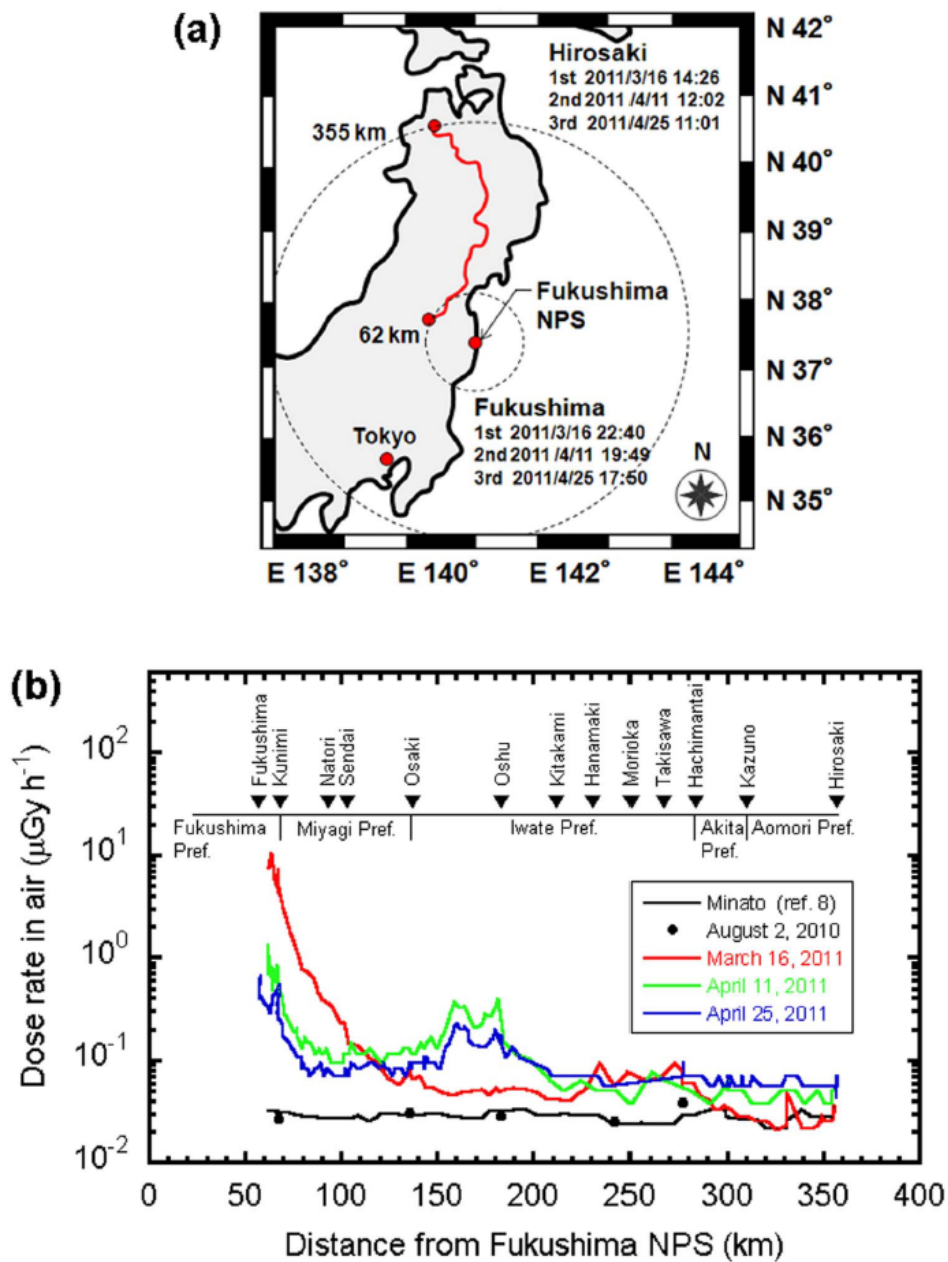


Figure 13. (a) Expressway survey route for measuring dose rates in air from Hirosaki City to Fukushima City. The starting point on March 16 and April 11 was Hirosaki City and on April 25 it was Fukushima City. Total distance on the expressway was 1256 km. (b) Temporal variation of dose rates in air before and after the start of the Fukushima crisis. The black line shows the dose rate in air reported by Minato8 in 2006. The solid black symbols are dose rates in air measured on August 2, 2010. The red, green and blue lines are dose rates in air measured on March 16, April 11 and April 25, 2011, respectively (Hosoda et al. 2012).

(Readings of air dose monitoring inside 80km zone of Fukushima Dai-ichi NPP)

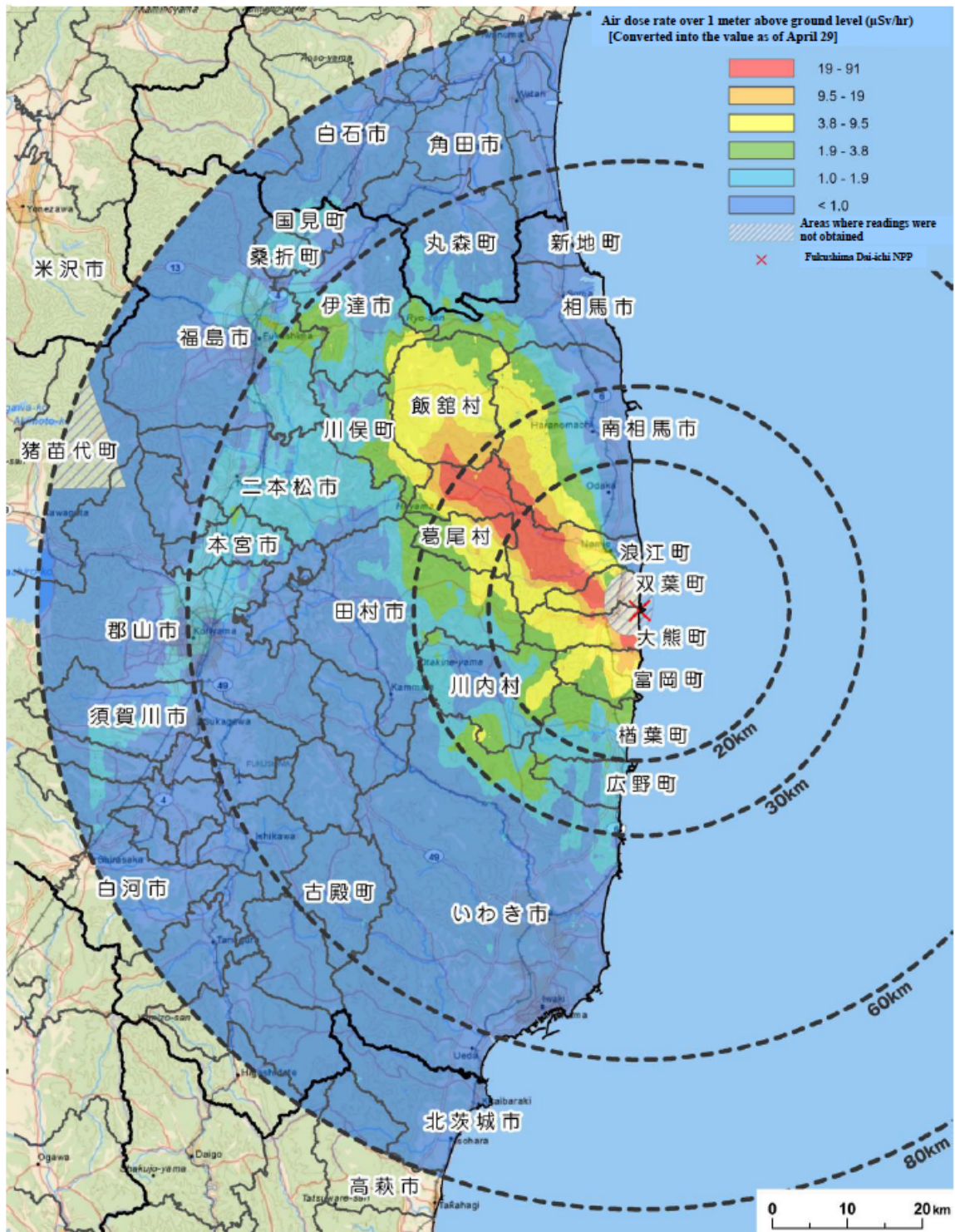


Figure 14. Results of airborne dose monitoring (Ministry of Education, Culture, Sports, Science and Technology and the U.S. Department of Energy, 2011).

(Total surface deposition of Cs-134 and Cs-137 inside 80 km zone of Fukushima Dai-ichi NPP)

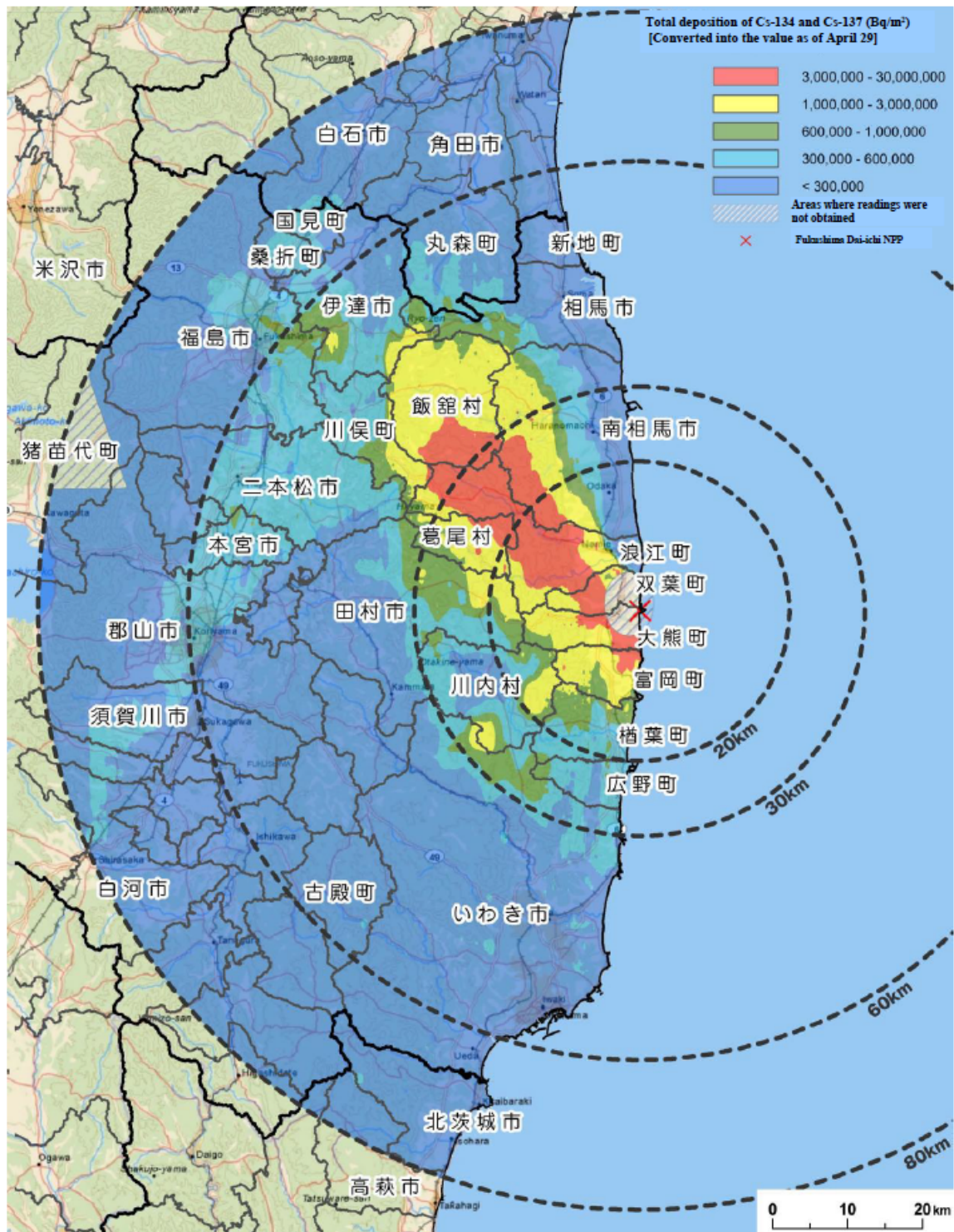


Figure 15. Results of Cs-137 and Cs-134 deposition monitoring (Ministry of Education, Culture, Sports, Science and Technology and the U.S. Department of Energy, 2011).

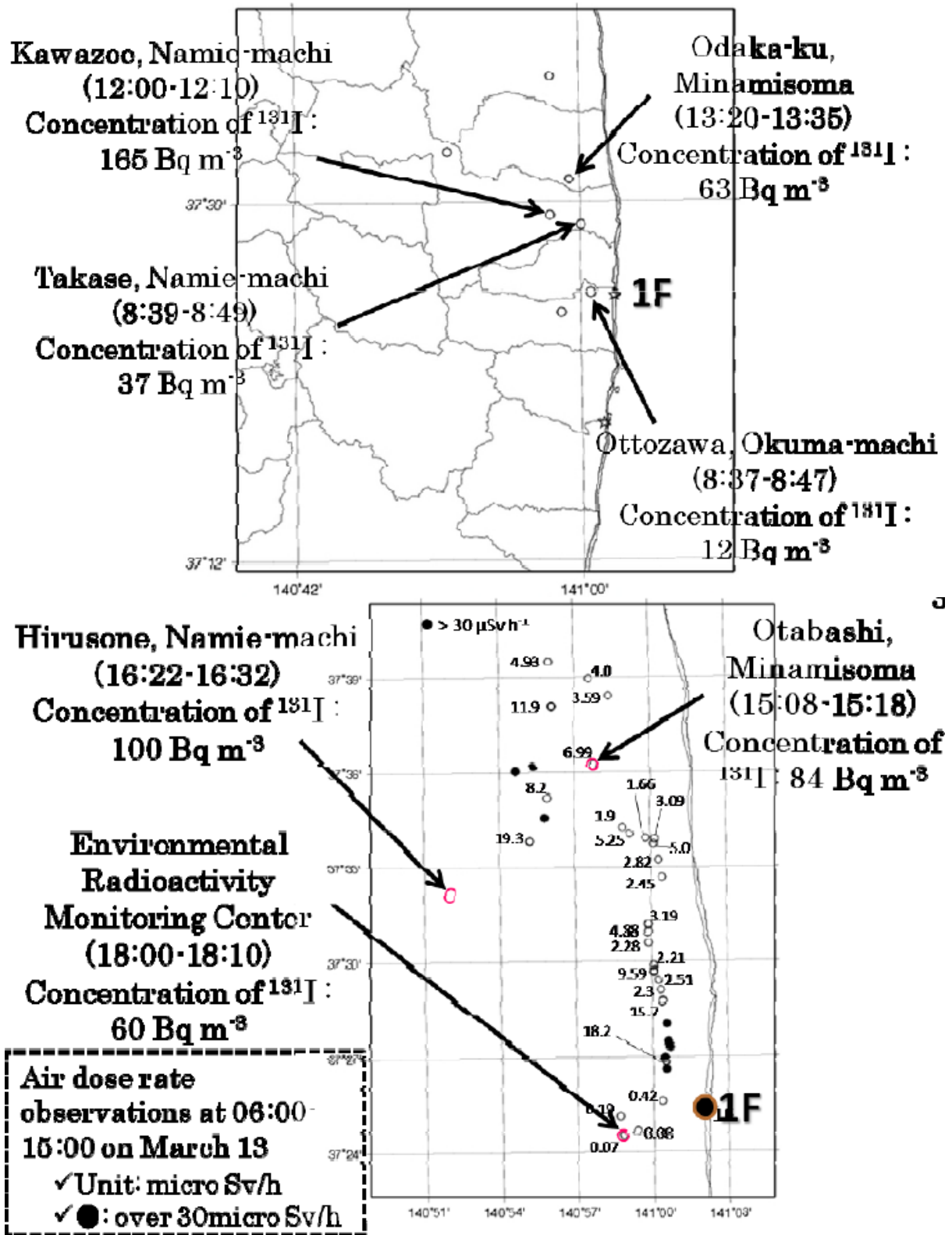


Figure 16. Measured I-131 concentrations and dose rates on March 12 (top) and March 13 (bottom) as reported by Nagai et al. (2012), apparently the time given is UTC.

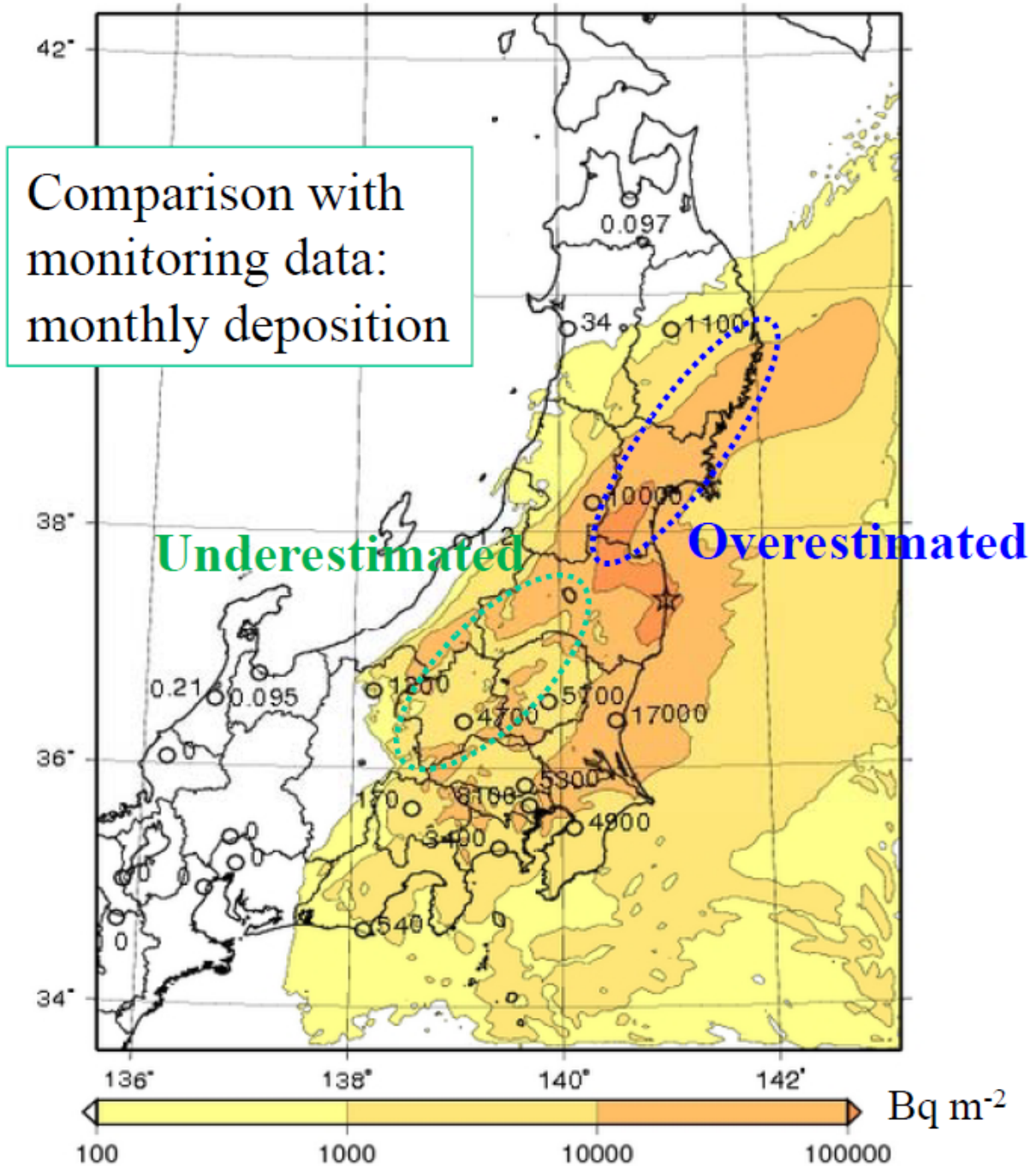


Figure 17. Monitored deposition of Cs-137 until the end of March 2011 according to Nagai et al. (2012).

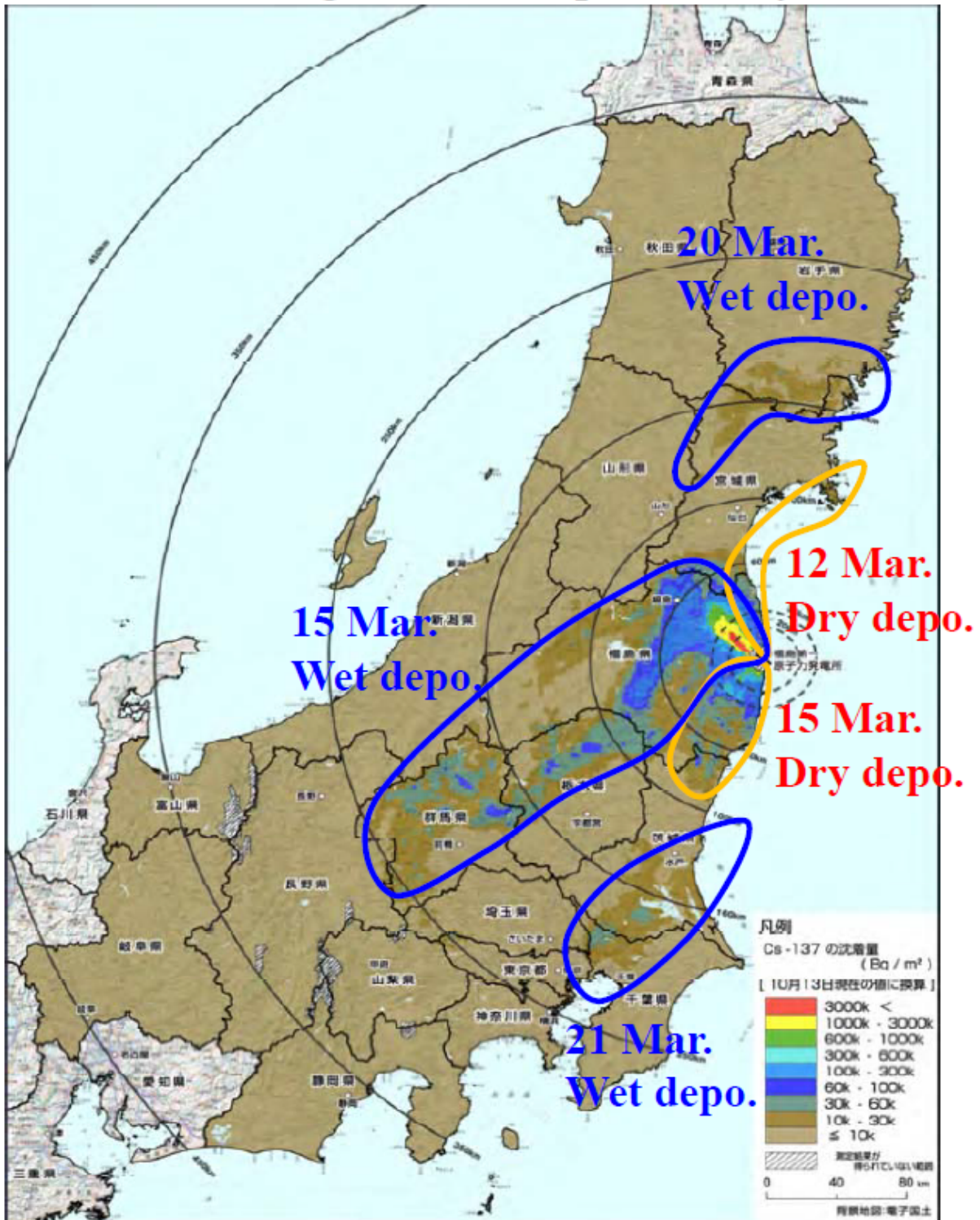


Figure 18. Monitored deposition of Cs-137 according to Nagai et al. (2012).

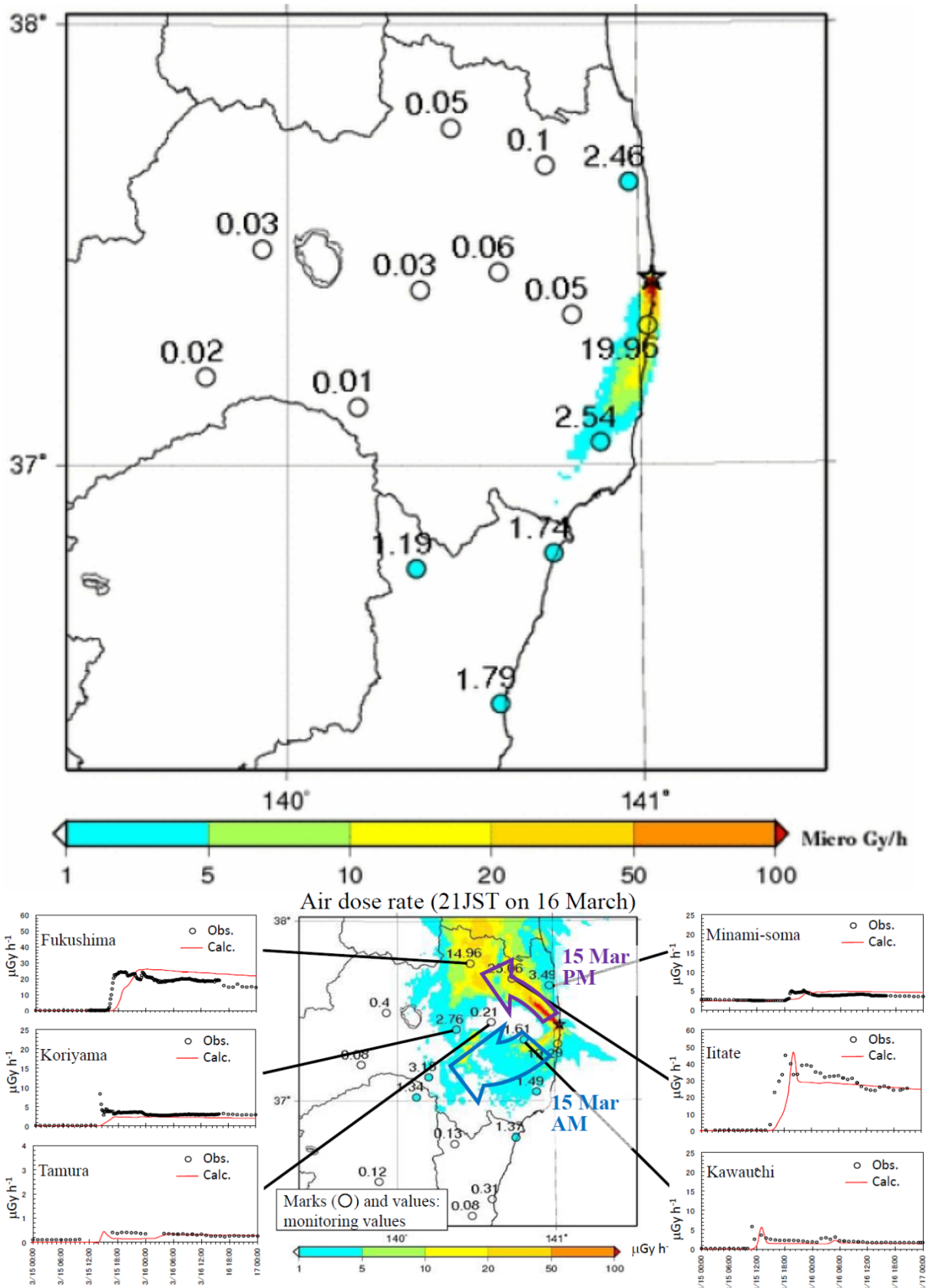


Figure 19. Dose rates on March 15 at 00:00 UTC (top) and dose rates in the high dose rate zone with temporal trends at different monitoring points (bottom). The points marked with **O** indicate monitoring results and the shaded area simulation results by SPEEDI-MP (Nagai et al. 2012).

5. ROSA simulations

The ROSA code (Interactive Real-Time Radiation Dose Prediction System) is based on the PSA-level 3 calculation code ARANO (Assessment of Consequences of Reactor Accidents and Normal Operation). The code fulfils the requirements and general specifications for the fast, interactive, real time dose calculation tool for emergency preparedness applications stated by the utilities in Finland. In addition the code system should work in completely automatic real-time mode utilizing the measured data of the pertinent power plant.

5.1 Main features of the code

- Straight-line trajectories with ordinary Gaussian model for horizontal dispersion
- Vertical concentration distribution solved from diffusion equation (so called Kz-model)
- Dry deposition described by the physically more realistic approach - surface depletion model instead of the usual source depletion approximation
- Solutions for vertical distribution taking into account disturbance by dry deposition (as a boundary condition) stored in comprehensive direct access data files (for different stability conditions, release heights and distances)
- Similarly the pre-calculated (3d space integration) values for normalized cloud shine doses are stored in DA-data files
- In dose calculations for specific conditions interpolation from these data files is performed
- Consequently significant simplifications have not been necessary for the new interactive, real time application to obtain sufficient calculation speed.

5.2 Source term

Three alternative specification modes of source term:

1. Based on readings from activity release monitors in real time (default operation mode of ROSA)
2. Pre-determined types of accidents with option to modify individual parameters like scaling of releases of all nuclides or nuclides in a certain group by same factor; in core melt accidents the relevant data is transmitted into the menu
3. Individually "tailored" releases by giving releases separately for each nuclide (max 84), or release fractions for fixed nuclide categories (noble gases, iodines etc)

Number of subphases and release heights:

- In mode 1: continuous follow-up; individual phases of release have a duration of 10 minutes

- In mode 2: pre-calculated releases can be divided up to a large number of subphases and each phase can have two release heights, in core melt accidents the number of subphases depends on the duration of the release (max 2 phases)
- In mode 3: max. 2 subphases and 2 release heights

5.3 Atmospheric dispersion

- Information on prevailing weather conditions automatically from meteorological mast (default mode) or specified by user
- For each subphase of release the dispersion direction can be individually chosen in modes 2 and 3
- In source term mode I, the code will use a certain updating interval of 10 minutes
- Each subsegment of the release plume continuous its transport to the original direction
- In longer duration releases additional horizontal dispersion by meandering is taken into account
- Building wake effects close to the source will be taken into account by fixed default parameter specifications

5.4 Exposure pathways

Total doses until a certain time point and total dose rates are calculated.

- Inhalation
 - Effective dose (with integration time 50 years)
 - Child's thyroid
 - Inhalation "dose rate" (Sv/h) is calculated as a difference of doses brought about two inhalation time periods
- Cloud shine
 - Calculation takes into account finite plume size
 - Calculation employs a pre-calculated data file
 - Linear energy dependence; normalized dose multiplied by photon yield and energy dependent factors
- Ground shine
 - Time-dependent ground concentration is calculated and multiplied by pertinent dose factors
 - Analytic integration until time points specified by user

- For continuous releases (source term mode I) and multiple phase releases new (semi-analytic) integration algorithms are developed.

5.5 Input

In the input phase, the following choices are made

- model accident
- main parameters to choose details of model accident
- main assumptions
- most important (adjustable) parameters; e.g. scaling of releases

The modelled accident scenarios include

1. Loss of coolant accidents
 - further subdivision according to severity
 - mild release (activity in primary coolant & spiking)
 - medium release (gap activity partially released)
 - high release (severe core damage)
2. Leakage of activity from primary to secondary circuit
 - 2a. Rupture of primary collector of steam generator
 - 2b. Steam generator tube rupture
3. Spent fuel handling accident
4. Rupture in
 - gas treatment system
 - liquid waste tank
 - main steam pipe line outside the containment
 - primary water pipe line outside the containment
5. Category of WASH-1400 releases

5.6 Output

The model presents results both on map background (dose and dose rate) and in tabular form. Form of presentation is equidose or equidose rates and levels can be modified in the output phase of ROSA without the need to recalculate doses (dose rates).

- Also output pages for
 - a more detailed tabular form
 - source term and weather
 - measured radiation data in the site environment

5.7 Simulation of the Fukushima dose rates

After the Fukushima accident ROSA was used to estimate external dose rates measured and reported in the vicinity of the Daichi power plant. The purpose was to estimate radiation dose rate from the passing plume even in such a way that it would correspond to the measured value. It was found that the dose rate in the vicinity of the power plant is strongly dependent of the release fractions of the nuclide groups besides atmospheric conditions. In other words equal dose rate can be obtained with different combinations of source terms.

In this exercise the following modelling assumptions and input choices were used. Note that the calculation is rather preliminary.

- Fission product inventory is based on that of the Olkiluoto 1&2 BWRs
- Pasquill class (stability class) is D, wind speed 3 m/s
- Distance is taken as 200 m from the source of release (i.e. within the plant site) where the highest reported dose rate was as high as 400 mSv/h (March 14, 2011)
- Decay heat production 3 days after scram
- Assuming that the dose rate of 400 mSv/h is caused by the radioactive plume (and not the exposed spent fuel pools), it is further presumed that
 - all noble gases have been released from the reactors
 - release fraction of other nuclides was set to zero
 - release duration is one hour

The results of the ROSA simulation are presented in Table 7 which shows the dose rates from different exposure pathways on March 14, 2011 at 01:00. The distance from the source is 0.2-20.0 km. The maximum external dose rate is 0.15 Sv/h. This value can be compared to the measured value of 0.4 Sv/h. Note that the simulation was run before detailed information of the releases were available: the interpolated weather data has not been used and the source term estimate was based on the reported highest dose rates on March 14, 2011.

Table 7. Dose rates in the ROSA simulation.

| Distance / Pathway | Dose rate 0.2 km (Sv/h) | Dose rate 1.0 km(Sv/h) | Dose rate 5.0 km(Sv/h) | Dose rate 10.0 km(Sv/h) | Dose rate 20.0 km(Sv/h) |
|--------------------|-------------------------|------------------------|------------------------|-------------------------|-------------------------|
| External | 1.5e-1 | 4.6e-2 | 7.1e-3 | 2.9e-3 | 0.0 |
| From cloud | 1.5e-1 | 4.6e-2 | 7.1e-3 | 2.9e-3 | 0.0 |
| Inhalation | 3.8e-10 | 2.6e-10 | 1.2e-10 | 5.8e-11 | 0.0 |
| Fallout | 2.8e-10 | 1.9e-10 | 6.7e-11 | 7.1e-12 | 0.0 |
| Child's thyroid | 2.6e-11 | 1.9e-11 | 3.2e-12 | 4.1e-12 | 0.0 |

6. VALMA simulations

VALMA is a dispersion and dose assessment code for accidental atmospheric radioactive releases (Ilvonen, 2002). It was developed at VTT in late 1990's and its main purpose was to serve as an emergency preparedness tool for radiation safety authorities (STUK in Finland). In such use, it is essential to produce predictions of concentrations, depositions, dose rates and doses in a reasonably short time to enable possible rapid countermeasures. It is not possible to perform CFD-like calculations that may last hours or days. Furthermore, it is possible that the best existing weather data cannot be received due to e.g. increased web traffic. For this reason, VALMA was made flexible enough to work with many kinds of weather data, starting from single-point measurements at the weather mast of an NPP (or several masts) and ending with Monte Carlo particles (even a limited number) that can be calculated, based on NWP models, with the SILAM dispersion model at FMI. Regardless of the source of weather data, VALMA offers the flexibility to calculate with changing source term estimates, including released nuclide inventory and the temporal and height distributions of different nuclides. It is also easy to set the spatial and temporal grids and to view the Lagrangian trajectories and dozens of result quantities on map or as temporal trends at chosen locations.

In short, VALMA works by dividing the release into a finite number of 'packets' or 'puffs', each of which corresponds to a 'slot' in time and release height. For each packet, VALMA computes a possibly winding central trajectory, which the packet will follow according to available wind information. VALMA follows each packet along the trajectory and calculates its spread, chain decay and deposition scavenging at the same time. VALMA calculates dozens of radiologically interesting quantities, like concentrations, depositions, dose rates and doses via different exposure pathways, together with their time derivatives and integrals. In contrast to an Eulerian dispersion model, VALMA uses a grid only to represent and accumulate the result quantities, not for calculating them.

6.1 Code description

The main program of VALMA is called `vtt_separate_program`. In typical use, it calls the subroutine `do_separate_dose_assessment`, which performs the actual calculations for one 'calculation case'. A calculation case is defined to be one certain combination of weather (function of place and time), source term, specification of requested results, and internal parameters of the calculation program. These are contained in the main input files of VALMA. Thus, a calculation case is a fully deterministic case, directly corresponding to e.g. an accident that has happened at a specific nuclear power plant at a specific time with a specific, known release of radioactive nuclides into the atmosphere (source term).

It is also possible to use VALMA for non-deterministic runs. These include e.g. probabilistic consequence assessment (PCA), uncertainty analysis, sensitivity analysis, feedback from field measurements using an iterative dose assessment loop, and studies of CPU (central processing unit) time usage. Each of these probabilistic assessments is programmed as a Fortran 90 (f90) module of its own, and the main subroutines of these modules are called by `vtt_separate_program` as needed. Then it is the task of the probabilistic subroutines to call the basic one case `do_separate_dose_assessment`. For example, when studying CPU time usage, the subroutine `produce_cpu_time_file` is called by `vtt_separate_program`.

The calculation of one case proceeds essentially in the following manner: particle trajectories (3D paths of hypothetical representative contaminant particles released into the atmosphere) are read from the intermediate file one at a time. Note that these paths will hereafter be

referred to simply as 'trajectories', even though they contain random movements in typical particle model style. Usually, the word 'trajectory' is reserved for non-random paths in the atmosphere. A set of nuclides with known activities in Becquerel [Bq], hereafter referred to as the 'nuclide cocktail' or simply 'cocktail', is attached to the trajectory. Calculation proceeds forwards in time along the trajectory. Several physical processes are calculated at each time step. The final result quantities are also calculated at each time step and stored in the result arrays, from where they are written into result files at the end of the calculation.

6.1.1 Input and other initialization

To understand the high level flow of VALMA calculation, the most crucial point is to understand the subroutine `do_separate_dose_assessment`. In this chapter, only a general overview of it is given. The various subroutines called by it will be handled in more detail later in this text. First of all, two key data structures, grid and source term, are acquired from their corresponding input files by `read_dose_input`. Subroutine `initialize_nuclides` determines the possible daughter nuclides of all nuclides appearing in the source term and retrieves the necessary data for all used nuclides from SILAM nuclide database. All used nuclides together make up the nuclide cocktail (`current_cocktail`). The set of nuclides will remain the same during one calculation case, but their amounts are constantly subject to change.

A very important part of the source term input file is the matrices that describe the 2D distribution of the release rate [Bq/s] of each nuclide in time and height. These matrices will hereafter be referred to as source strength matrices, or SSMs. The elements of an SSM do not have a unit, but they are merely relative values relative to each other inside one certain matrix. For each starting trajectory, the source strength values of all nuclides are calculated by interpolation in time and height from their corresponding SSMs. The actual values generated by this procedure are dependent on the actual starting times and heights appearing in the set of trajectories used. However, the final values to be used must be real fractions of the total released amount, i.e. their sum has to be equal to one. For this reason, `do_separate_dose_assessment` calls `src_strength_normalization`, which sweeps through the complete set of trajectories before the actual calculation starts and determines the source strength normalization factors.

In some cases, the actual spatial and temporal grids used in the calculation might not be those specified by the user in the grid specification file (default name `grid_spec.in`). The actual grids are determined by `final_choice_of_grid`. After this, it is possible to allocate memory for result quantities. Only the exact amount of memory needed is allocated. The arrays of the result quantities are by far the biggest arrays in VALMA, so it is very important that no memory space is wasted in them. Smaller arrays in VALMA usually have parameterized bounds defined at compilation time.

6.1.2 Particle trajectories and calculation time steps

As soon as memory has been allocated, the real 'kernel' of VALMA starts working. At the highest level in `do_separate_dose_assessment`, the kernel only comprises some 40 lines of source code. It has two nested loops, the outer of which goes through all the particle trajectories, and the inner one goes along one trajectory in calculation time steps. This order is made possible by the fact that particles are independent from each other, and their total effect results from simple superposition.

The handling of one trajectory starts with a call to `fu_get_next_trajectory`, which returns as a data structure the next unused trajectory contained in the current set of trajectory files. (Note that in the whole SILAM, all function names start with `fu_` to better distinguish them from array names.) The amounts of nuclides in the current nuclide cocktail are then initialized using the starting time and height of the trajectory. If the released amounts in the source term

specification file (default name `source_term.in`) refer to the time of the reactor SCRAM (shutdown of a reactor; fission stops), they are put subject to radioactive chain decay for the time period between SCRAM and the starting time of the trajectory by calling `do_decay_of_cocktail`.

When the initial cocktail is ready, the time step loop starts. Calculation is not dependent on the time step between successive trajectory points in the VALMA SSDA intermediate file (trajectory file or a set of trajectory files). The trajectory points may well have arbitrary, even variable temporal spacing. Smallest time step might be applied over most interesting target areas. A so called virtual trajectory point is calculated by linear interpolation along the trajectory. The internal time step of dose calculation must be smaller than the time step between successive trajectory points in order to guarantee to utilize all available information.

The call to `recursive_quantities` returns such values that cannot be calculated using the present virtual point only, but also information from history is needed. The length of last time step and ρ_y , the lateral standard deviation of the position of a contaminant particle according to assumed Gaussian distribution are such 'recursive quantities'. Note that the Gaussian distribution is the basis of many very simple dispersion models. SILAM is not a Gaussian dispersion model, although some ideas from such models are utilized in SSDA and VALMA.

6.1.3 Calculation of the result quantities of dose assessment

After calculating recursive quantities starts the most important section of the VALMA kernel. It performs the following steps:

- The nuclide cocktail is put subject to radioactive chain decay during the calculation time step
- The result quantities (atmospheric concentration, deposition, dose rates and doses) are calculated for each nuclide
- All result quantities are added to their values already present in the final result arrays

Note that the words deposition and fallout are both used to describe the activities per area on ground surface in [Bq/m^2]. The processes bringing nuclides from the cloud to the ground are referred to as deposition processes. The word fallout is usually used in connection with further physical quantities, e.g. 'fallout gamma dose rate'.

The result quantities associated with the current virtual point are calculated by subroutine `calculate_current_quantities`. It handles deposition processes, but assumes a uniform horizontal distribution in the currently considered relatively small area. The quantities are returned in the array `current_quantities`, whose indices mean dose pathway, physical quantity and nuclide. A 'dose pathway' is here defined as a combination of exposure or intake mode (cloudshine or submersion, groundshine from fallout, inhalation and ingestion), possibly target organ and possibly integration time. Physical quantity may be one of concentration type quantities, dose rate or dose. Some elements of `current_quantities` may remain unused, whenever a certain combination of pathway, quantity and nuclide is not applicable. Note that there is no index for time in `current_quantities`. Instead, internal doses for various integration times are handled as separate pathways, and fallout gamma doses are explicitly integrated up to any later time point requested by the user at a later stage (using complete information on nuclide cocktail).

6.1.4 Transformation into grid representation

When the current quantities have been calculated, they are added in the final result arrays using tools from the module `particles_to_grid`. There are two such dynamically allocated final arrays, `result_array` for results in regular grid, and `point_results` for results at arbitrarily scattered points. Their indices mean quantity, coordinates in longitude and latitude directions (or just the index of a point), and index of time step. In this context, a 'quantity' means a combination of all the indices of `current_quantities`. Note that there is no separate index for height, because in usual dose assessment applications all results refer to values of quantities at a level near ground surface. If a certain result quantity is wanted for several different heights, these have to be defined as separate quantities.

Subroutine `put_quantities_into_final_grids` takes care of correcting the horizontal distribution from uniform to Gaussian, when this is requested. Note that with a large number of particles it is usually best to use horizontally uniformly distributed, relatively small circular or even rectangular 'areas affected by particle'. On the other hand, VALMA is also capable of calculating even with one single particle (actually any number of particles is equally well possible). In that extreme case, large enough affected areas with Gaussian horizontal distribution should be used. With any number of particles, use of Gaussian distribution in the horizontal is theoretically justified, because the transformation task is actually that of determining the correct continuous distribution from the calculated discrete distribution having a finite number of sample particles; a usual approach in such cases is estimation of probability density by using Parzen windows and kernel functions.

The calculation of deposited amounts at future times and all further calculations based on them is also the task of `put_quantities_into_final_grids`. It performs these tasks using appropriate task specific subroutines.

As soon as the current quantities have been put into the final result arrays, the time loop moves to the next virtual trajectory point and calculations start all over again with `recursive_quantities`. When the trajectory ends, its contribution to the result quantity fields ends as well. The user will be informed on the last time point with complete trajectory data (i.e. the last time point that is reached by all trajectories in the given trajectory file). When the last trajectory has been calculated, the final result arrays are ready.

The 'post processing' of result fields by `do_separate_dose_assessment` includes some automatic checking (non-negativity etc.), a quick result report for the user, a subroutine call to write all output files, and finally deallocation of the dynamic arrays, which is necessary if another, possibly different sized calculation case will be the next in order.

6.1.5 Use of weather data measured by mast equipment

VALMA receives data on weather conditions either from SILAM (fresh or archived predictions) or from measuring equipment (current or archived measured values). The information content of SILAM data is typically many orders of magnitude more than that of measurements. For this reason, SILAM data should preferably be used. The only exception is dose assessment very near the source (distances less than some 15 km). However, this limit will probably be subject to continuous decrease as the HIRLAM model, from which SILAM gets numerical weather predictions, is developed and run on faster computers.

Measured weather data may come to VALMA from arbitrarily many measuring points, typically equipment installed at a certain height in a weather mast. A point is defined by its latitude, longitude and height from ground surface. Currently VALMA does not accept physical observations (temperatures, rain intensity) as such, but they have to be transformed to various derived quantities. VALMA reads measured weather data as wind direction and speed, stability class, mixing height and washout coefficient. In practice, it is recommended

to connect VALMA through a 'filter' program, deriving the necessary quantities, to raw weather mast data available on e.g. the plant computer of an NPP.

When using measured weather data, VALMA is essentially a 'puff model' like the classic and well-known Danish RIMPUFF. Just like with SILAM data, the release is divided into arbitrarily many pieces that start at successive time points. Each piece is transported along its own central trajectory. To have observations for all the spatial and temporal points needed for trajectory calculation, VALMA interpolates the original observations first in time, then in space. The spatial interpolation is a simple weighted average with weights of the form $1/r^2$. There are several obvious improvements that could be programmed into the interpolation, like leaving out a point that is approximately behind another one.

VALMA uses a simple, fully explicit method of trajectory calculation, which advances based on starting point data only and thus requires a short time step (does not however essentially affect the total CPU time of VALMA). It is fairly easy to program a more advanced method, like the so-called Petterssen iteration of SILAM, in VALMA code whenever so required. VALMA is able to use spherical trigonometry (instead of planar geometry), so even long distances can be handled anywhere on earth, provided that measuring points exist.

In VALMA, the puffs spread horizontally according to classical formulas of σ_y . Change of stability is handled with the so-called virtual source principle. Vertical dispersion can be selected from various methods, of which probably the best but slowest is the use of vertical profiles based on the K theory of turbulent diffusion, where dry deposition is included as a flux boundary condition.

6.2 Input

The input selections used in the modelling of the Fukushima accident are described below. The released activities for each nuclide are presented in Table 8.

- input file "source_term.in"
 - location: lat = 37.233 N, lon = 141.015 E
 - time of earthquake: March 11, 2011, 05:46:24 UTC
 - start of atmospheric release: March 12, 05:00:00 UTC (exact time is not known)
 - modelled duration of release: 30 x 24 h = 720 h
 - min & max release height: 20 m (0...40), 100 m (50...150)
 - SCRAM or measured activities: In VALMA, the user can select if the source term activity refers to the time of the reactor SCRAM (in which case VALMA will calculate the initial chain decay before release into the atmosphere according to given time delay), or if the activity refers to each actual piece of emission that exited from the containment.
 - nuclide contents & activities (Bq) and their combined temporal & height distributions
 - 37 most important nuclides taken into account (47 with decay chains)

- Temporal distributions
 - Noble gases according to Xe-133 by Stohl et al. (2012), (Figure 5)
 - All iodine isotopes according to I-131 by Nagai et al. (2012), (Figure 3)
 - All other nuclides according to Cs-137 of Nagai et al. (2012) (Figure 3)
- Release height set at 60 m (due to a minor technical restriction in the code in the subroutine of trajectory generation which could not be overcome in a reasonable working time)
- input file “tr_file_list.in”
 - “trajectory_files/generated.tmp”: This is the reserved file name that directs VALMA to calculate trajectories instead of expecting data from SILAM
- input file “weather_mast.in”
 - In this case, the mast is only virtually existing: lat = 37.422 N, lon = 141.031 E, measuring heights 20 m and 100 m
 - starting time and interval of measurements: March 10, 2011, 0:00 UTC; 3600s
 - spread direction, wind speed, mixing height, washout coefficient, stability class
 - mixing height as a function of stability class
- input file “grid_spec.in”
 - given latitude and longitude bounds
 - lon1 lon2 nsteps: 139, 141.5, interval 2.5
 - lat1 lat2 nsteps: 35.5, 38, interval 2.5
 - first & last time point & time step: 1 h, 199 h, 1 h
 - observed stations’ geographical coordinates

Table 8. The source term in VALMA input: the released nuclides and their amounts.

| Nuclide | Activity (Bq) |
|-----------|---------------|
| 'I-131' | 1.60E+17 |
| 'CS-137' | 1.50E+16 |
| 'CS-134' | 1.80E+16 |
| 'XE-133' | 1.10E+19 |
| 'KR-85' | 3.00E+16 |
| 'KR-85M' | 2.70E+09 |
| 'KR-87' | 1.00E+14 |
| 'KR-88' | 7.80E+04 |
| 'I-132' | 7.40E+17 |
| 'I-133' | 4.10E+16 |
| 'XE-133M' | 4.40E+16 |
| 'I-134' | 1.00E+12 |
| 'I-135' | 4.10E+12 |
| 'XE-135' | 1.10E+15 |
| 'XE-135M' | 6.30E+12 |
| 'BA-140' | 4.80E+17 |
| 'CE-141' | 2.50E+16 |
| 'CE-144' | 2.20E+16 |
| 'CS-136' | 6.70E+16 |
| 'LA-140' | 3.00E+16 |
| 'NB-95' | 2.70E+16 |
| 'NP-239' | 7.40E+16 |
| 'PR-143' | 1.90E+16 |
| 'PR-144' | 2.20E+16 |
| 'RH-103M' | 1.90E+16 |
| 'RU-103' | 1.90E+16 |
| 'SB-127' | 3.00E+16 |
| 'SR-89' | 3.00E+17 |
| 'SR-90' | 2.50E+16 |
| 'TE-127' | 4.40E+16 |
| 'TE-127M' | 1.30E+16 |
| 'TE-129' | 3.30E+16 |
| 'TE-129M' | 5.20E+16 |
| 'TE-132' | 4.10E+17 |
| 'XE-131M' | 3.70E+16 |
| 'Y-91' | 1.80E+16 |
| 'ZR-95' | 2.50E+16 |

6.2.1 Weather data

The wind speed data used in the VALMA simulations is presented in the series of figures below: Figure 20 - Figure 25. The different colours indicate different dates, for example:

March 11 – blue

March 12 – green

March 13 – red

March 14 – cyan

March 15 – magenta

March 16 – yellow

March 17 – black

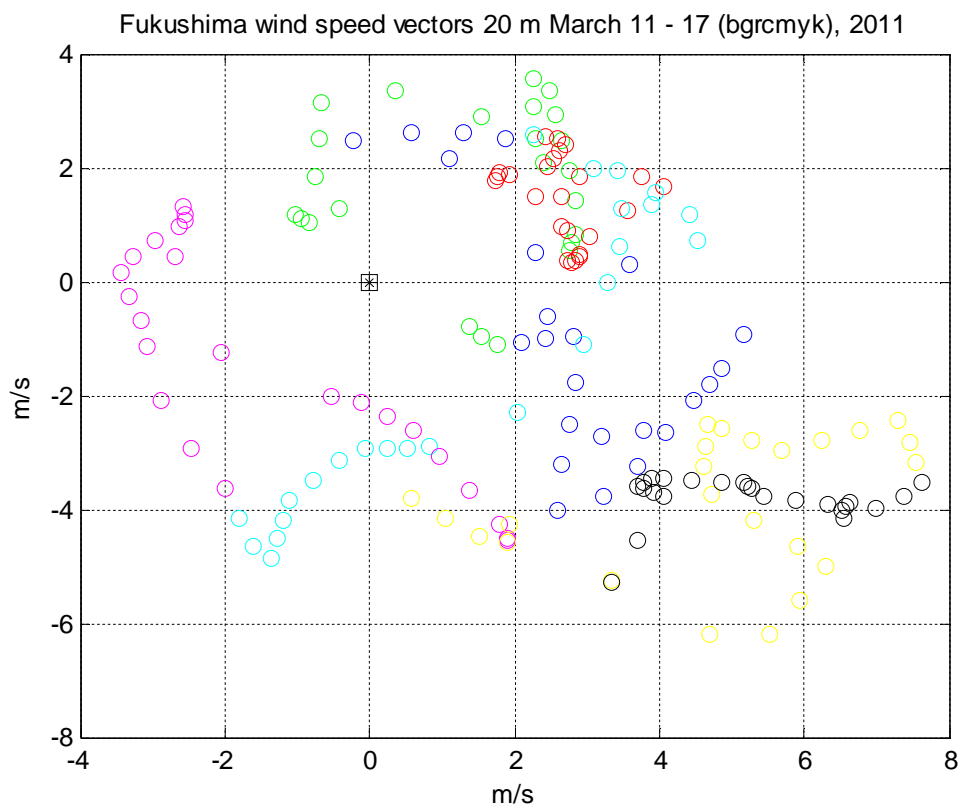


Figure 20. Wind speed vectors for March 11 -17, 2011, at 20 m height.

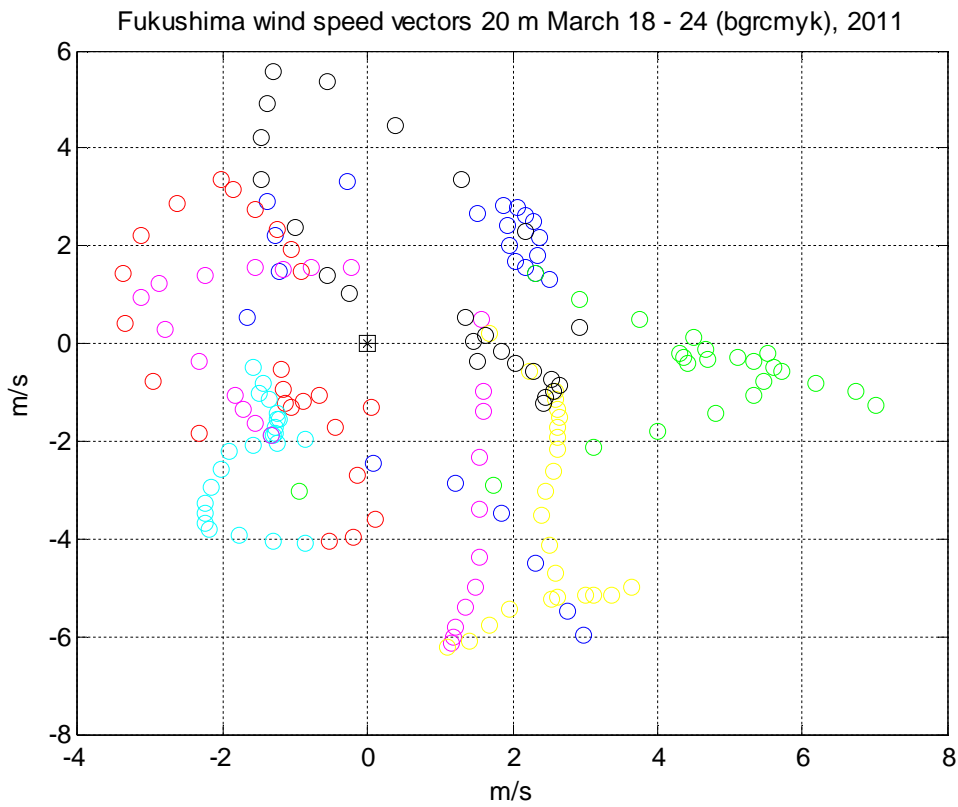


Figure 21. Wind speed vectors for March 18 -24, 2011, at 20 m height.

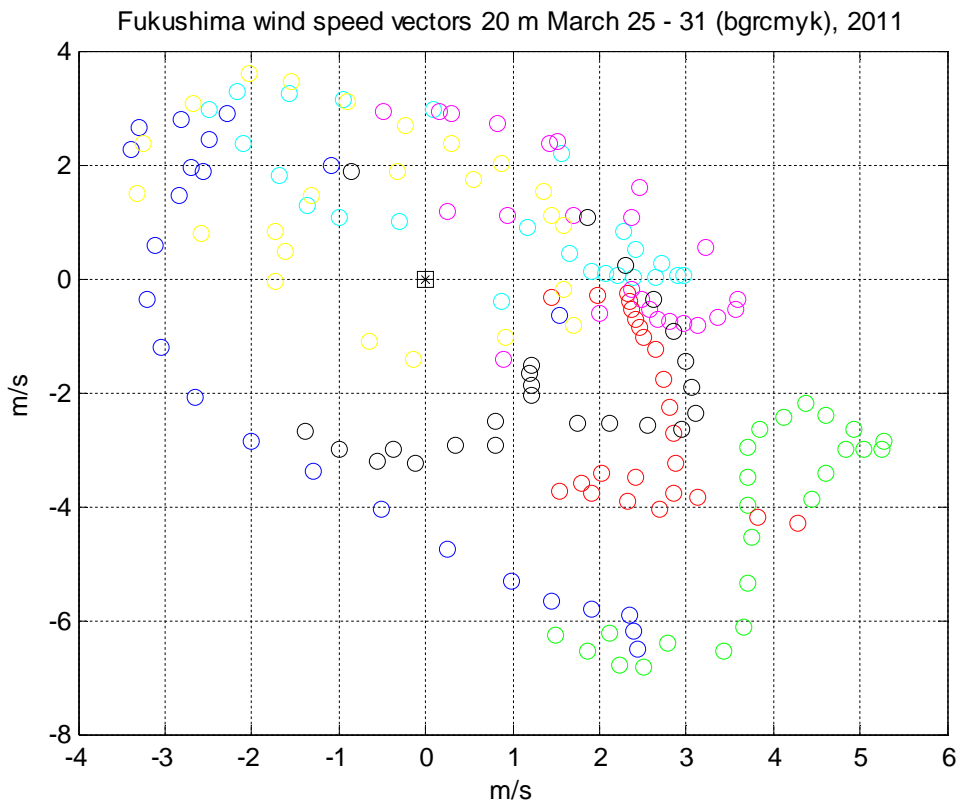


Figure 22. Wind speed vectors for March 25 -31, 2011, at 20 m height.

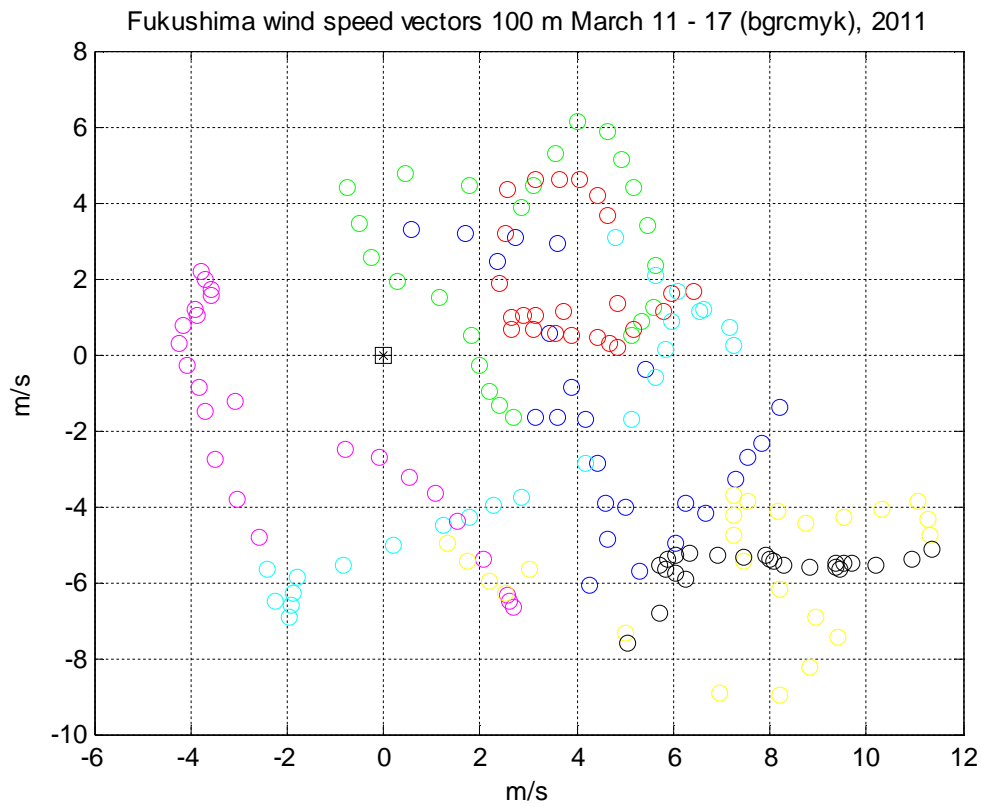


Figure 23. Wind speed vectors for March 11 -17, 2011, at 100 m height.

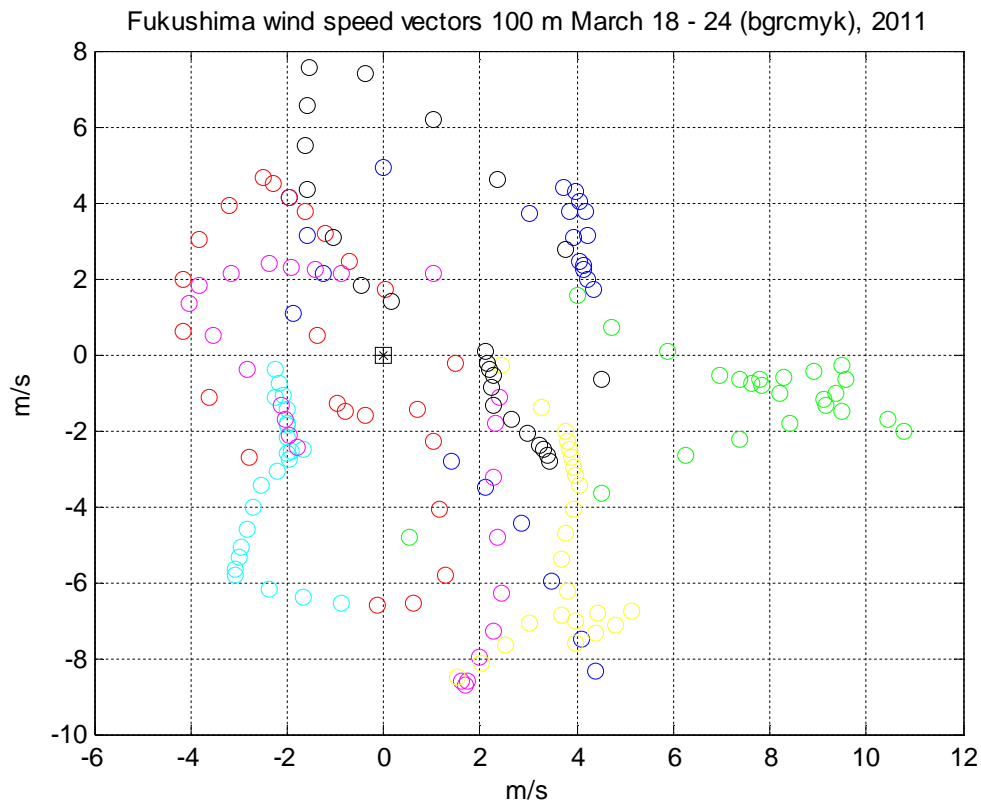


Figure 24. Wind speed vectors for March 18 -24, 2011, at 100 m height.

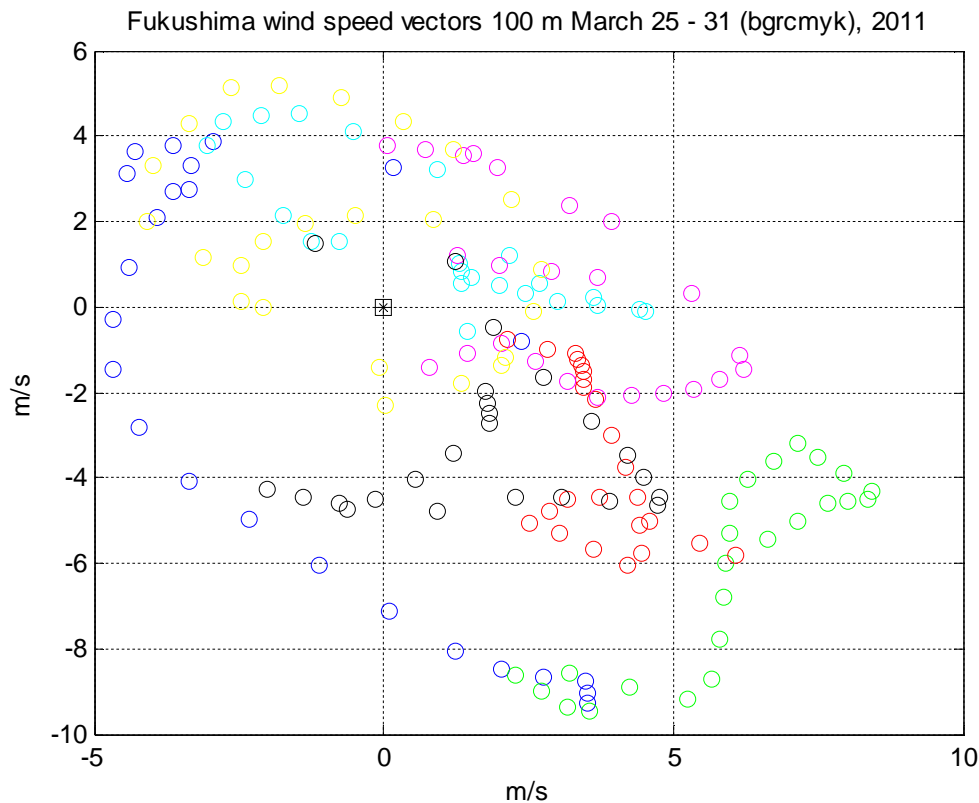


Figure 25. Wind speed vectors for March 25 -31, 2011, at 100 m height.

6.3 Results

The main results of the VALMA calculations are presented in this Section. They include caesium and iodine air concentrations, Cs deposition and dose rates during the investigated period.

6.3.1 Particle trajectories

Particle trajectories calculated by VALMA from the Fukushima one-point weather data are shown in Figure 26. There are 721 trajectories starting at 1 h intervals, first one at 05:00 UTC, March 11, 2011. Each trajectory was followed by VALMA until 20 h from its start. The trajectories are curved, because the one-point weather data is assumed valid even elsewhere. In practice, the transport is not always reliably calculated with one-point weather data even when only 10 km from the source.

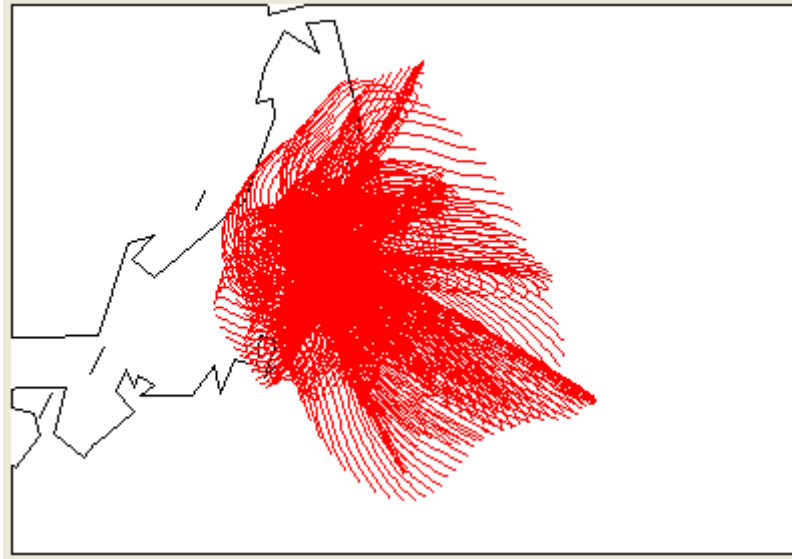


Figure 26. Particle trajectories calculated by VALMA from the Fukushima one-point weather data.

The SILAM parameterization for calculation of washout coefficients has 3 branches: if height (pressure level) is more than 900 hPa, the point is assumed to be under the cloud, between 700 and 900 hPa inside the cloud, and for pressure levels less than 700 hPa, the washout coefficient is set to zero. Under the cloud, the washout coefficient can be calculated as

- $Is_{scav} = pr_{Is}^{0.79} * 0.05417$

where pr_{Is} is rain intensity as mm/s (or kg/m²s). There are some differences for snow and for the rainout coefficient in convective rain.

6.3.2 Concentrations

The iodine concentrations predicted by VALMA are illustrated in the sequence of maps in Figure 27 - Figure 29 and the caesium concentration in Figure 30. The size of the map grid shown in the figures is 45 x 45 km. There is some “zebra striping” visible in VALMA results but this is not an artefact of simulation algorithms as such, it is due to too long time steps. The time steps were intentionally kept long for practical reasons.

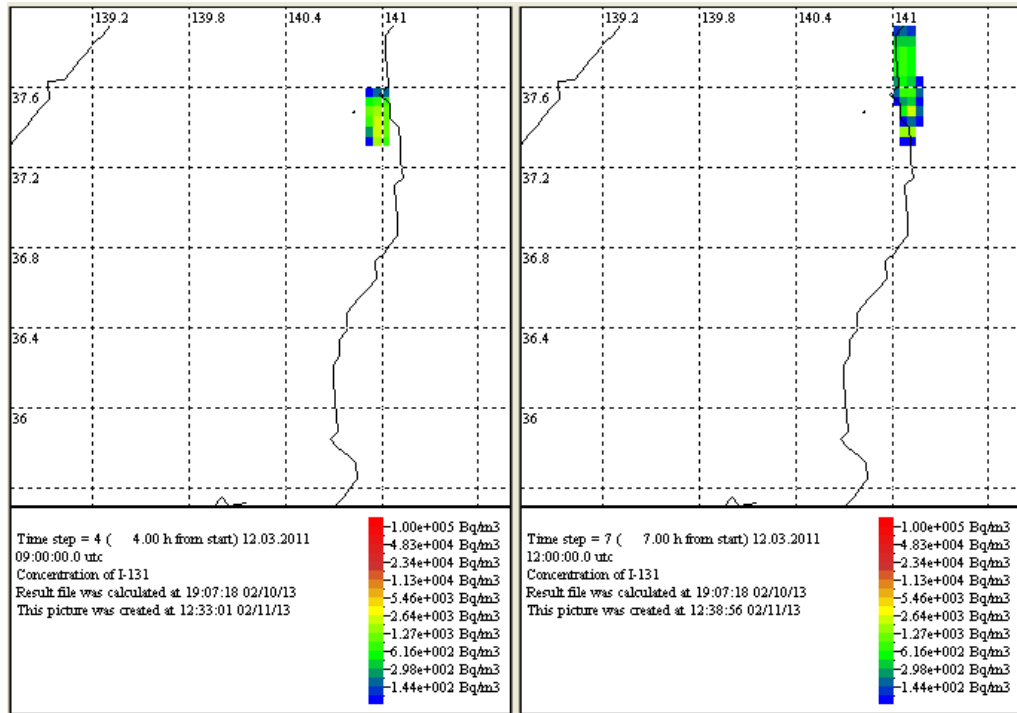


Figure 27. I-131 concentrations on 12.03.2011 at 09:00 UTC (left) and at 12:00 UTC (right).

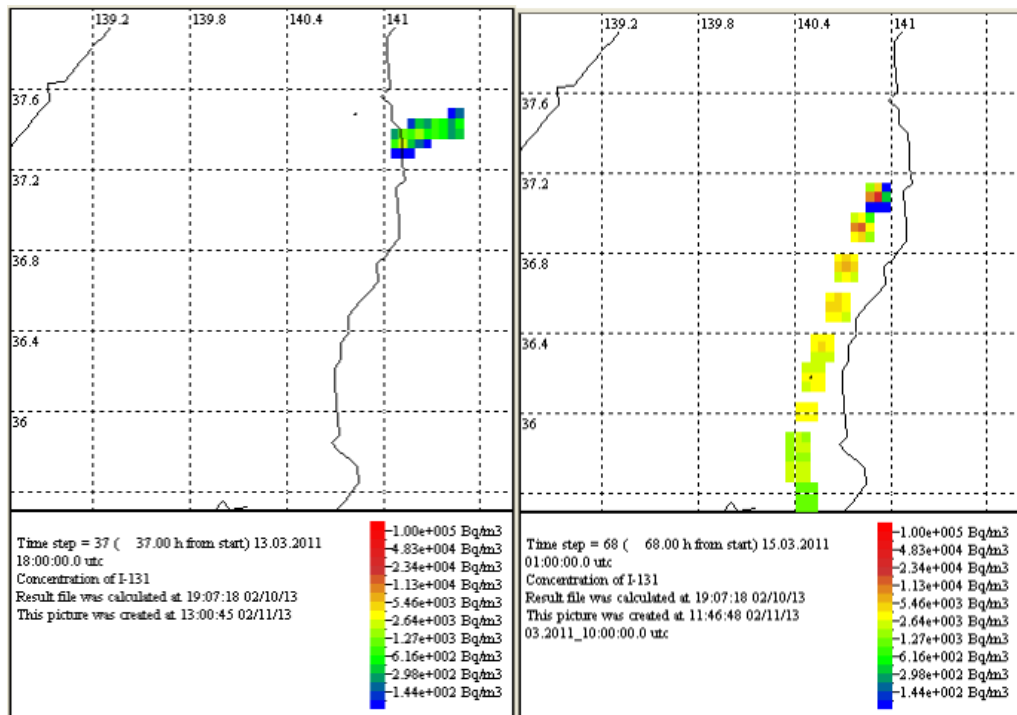


Figure 28. I-131 concentrations on 13.03.2011 at 18:00 UTC (left) and on 15.03.2011 at 01:00 UTC (right).

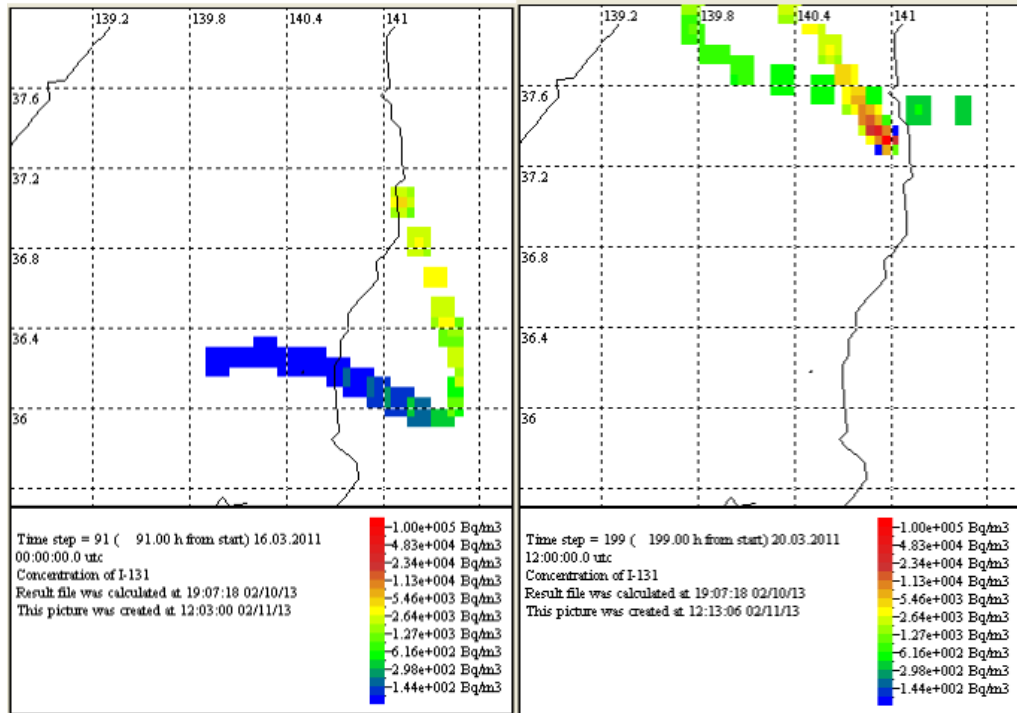


Figure 29. I-131 concentrations on 16.03.2011 at 00:00 UTC (left) and on 20.03.2011 at 12:00 UTC (right).

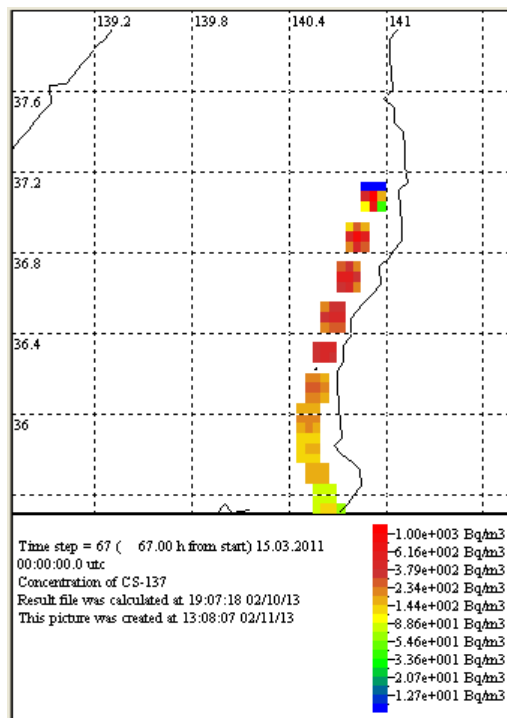


Figure 30. Cs-137 concentration on 15.3.2011 at 00:00 UTC.

6.3.3 Depositions

The ground depositions of caesium are shown in the maps in Figure 31 - Figure 32.

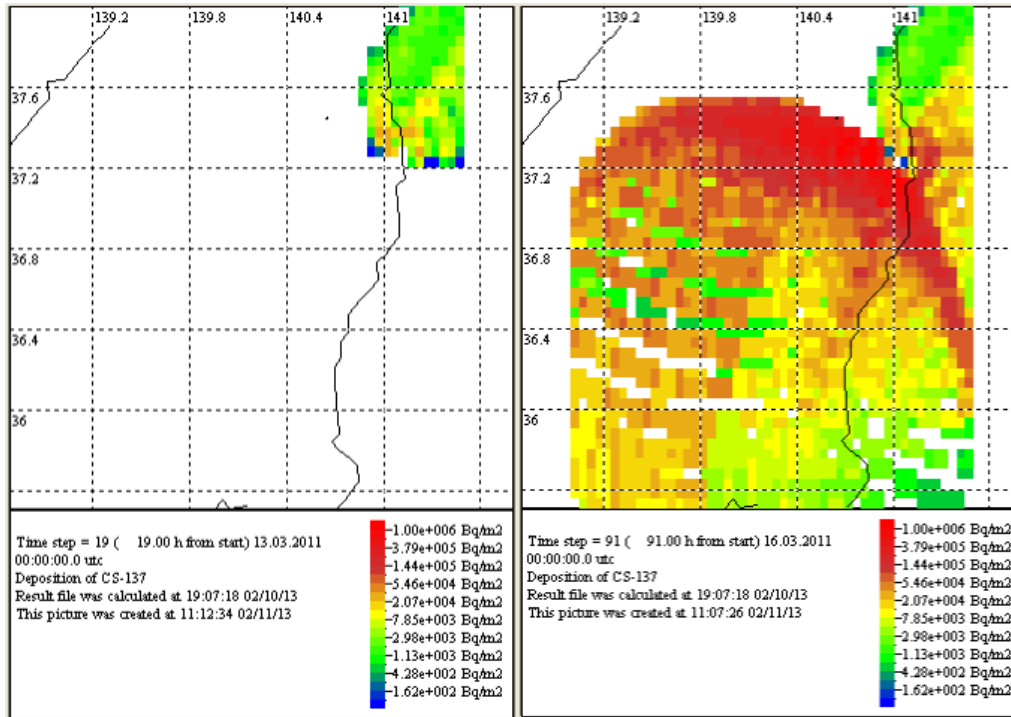


Figure 31. Cs-137 depositions on 13.3.2011 at 00:00 UTC (left) and on 16.3.2011 at 00:00 UTC (right).

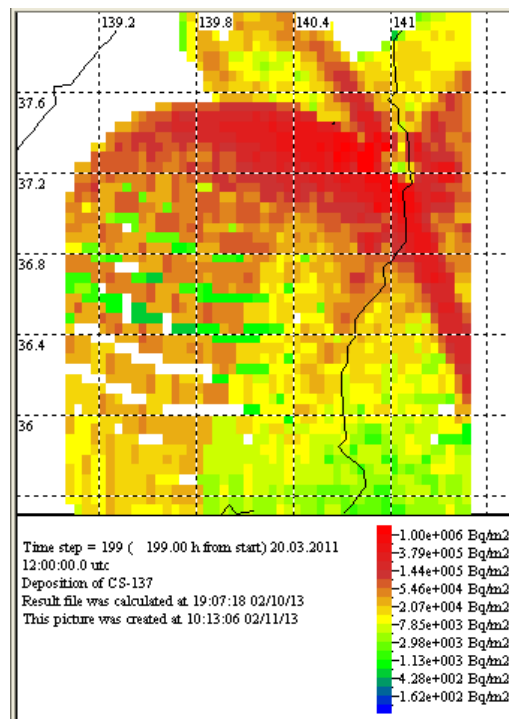


Figure 32. Cs-137 deposition on 20.3.2011 at 12:00 UTC.

6.3.4 Dose rates

The external dose rates on March 15-16 according to the VALMA calculation are illustrated in Figure 33 and Figure 34.

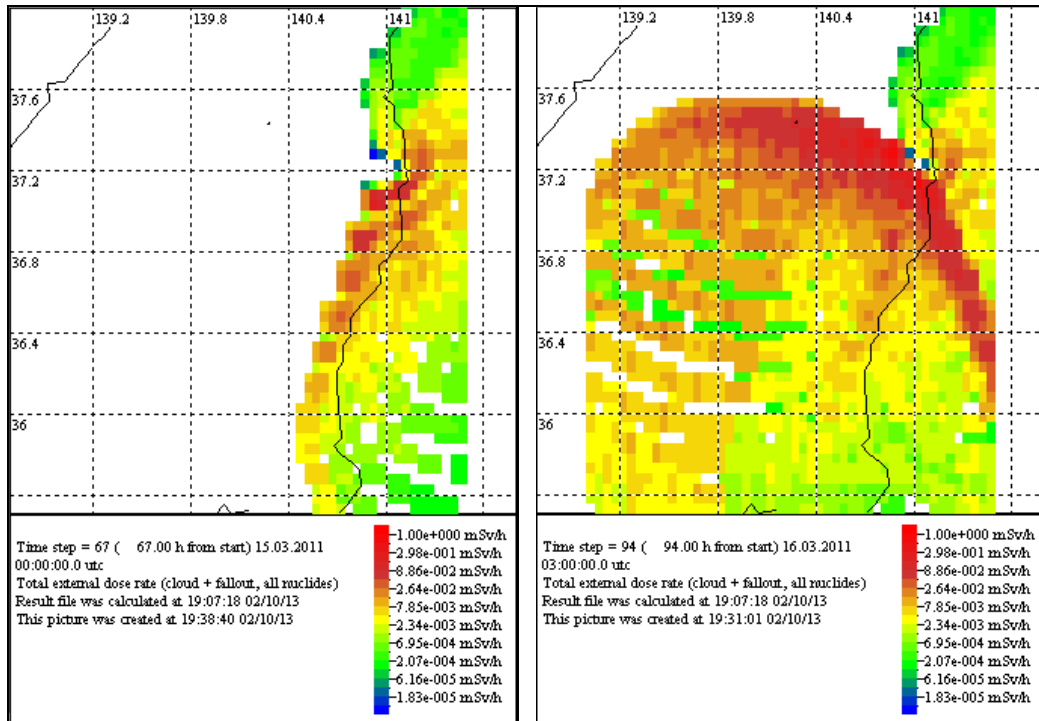


Figure 33. Total external dose rate on 15.3.2011 at 00:00 UTC (left) and on 16.3.2011 at 03:00 UTC (right).

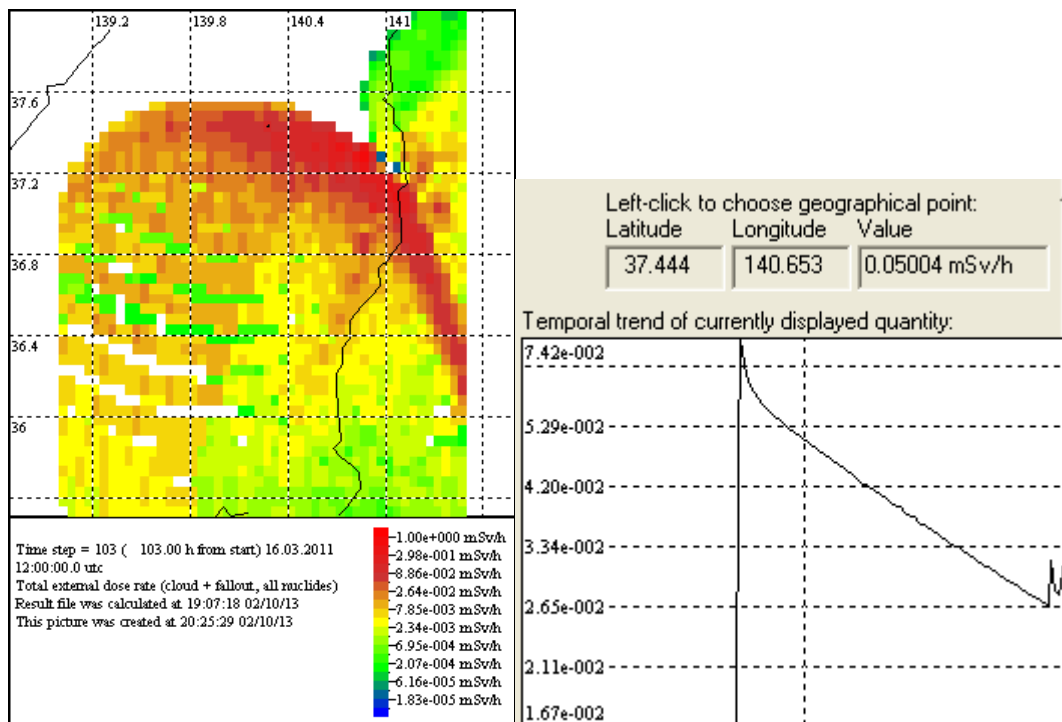


Figure 34. Total external dose rate on 16.3.2011 at 12:00 UTC (left) and the time history of dose rate at 37.4°N, 140.6°E during the simulation, 0 – 199 h (right) .

7. Other simulations

An example of dispersion simulations found in the literature (Stohl. et al. 2012) is shown in Figure 35. According to this simulation, the highest total deposition (by the end of April) is found northwest of the plant site, generally in the same direction as the main deposits predicted by VALMA until March 20. According to Stohl at al. (2012) the simulation results are in accordance with monitoring surveys.

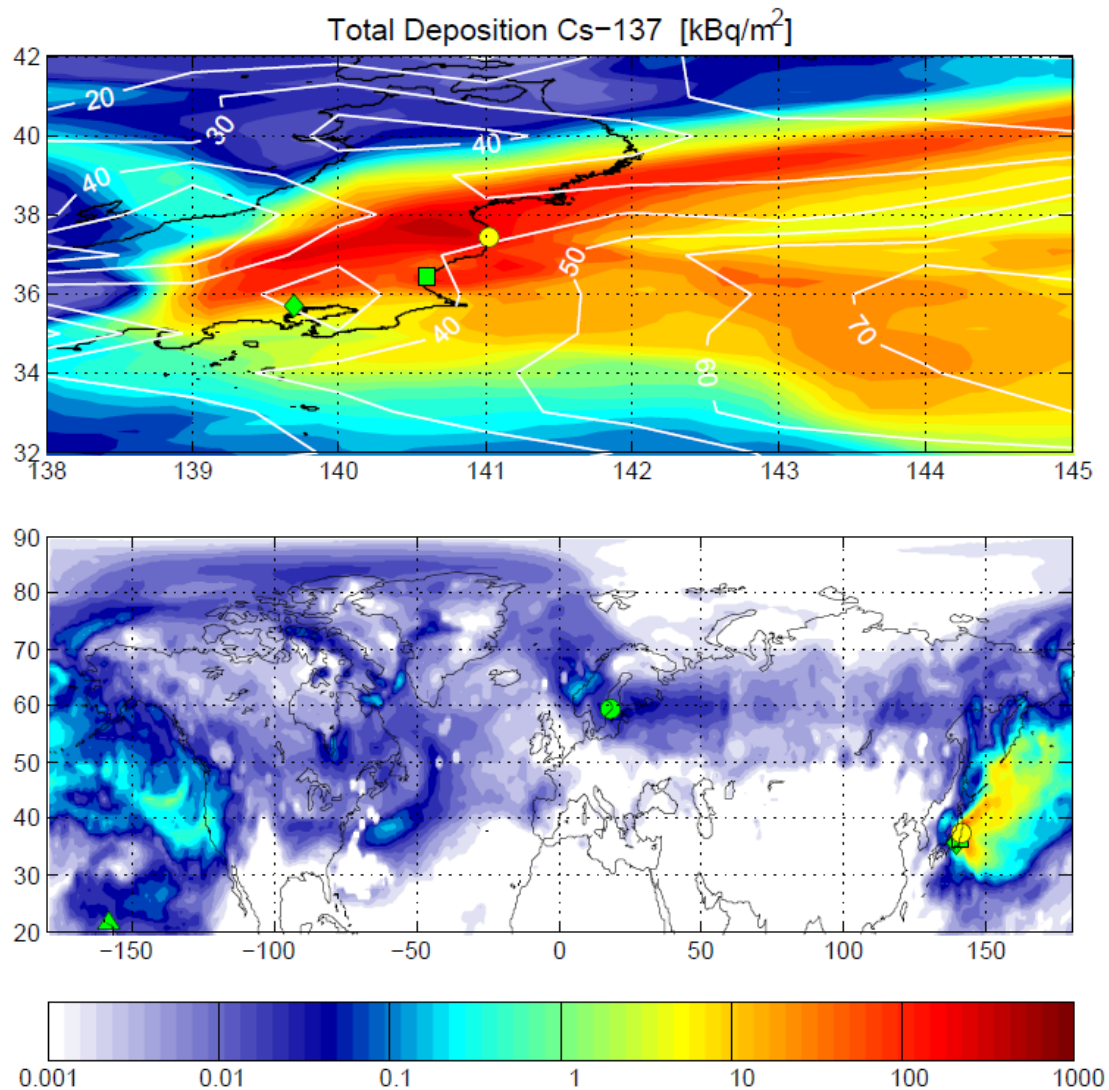


Figure 35. Maps of total deposition of Cs-137 until 20 April 00:00 UTC, for Japan (upper panel) and the global domain (lower panel). Superimposed on the upper panel is the total precipitation from GFS for the same time period. The location of FD NPP is shown with a yellow circle, the air sampling site Tokai-mura with a green square, and the deposition monitoring site in Tokyo with a green diamond. In the lower panel, the stations Oahu (Hawaii) and Stockholm (Sweden) are marked with a green triangle and a green circle, respectively (Stohl et al. 2012).

8. Discussion

A variety of measurements and simulations concerning the radionuclide dispersion and the resulting air concentrations, fallout and dose rates have been reported by different authors. Readings from monitoring points and different types of surveys during and after the accident have been reported e.g. by MEXT. The Fukushima monitoring database made available by the IAEA contains the radiological monitoring data that was officially reported to the IAEA during the emergency phase of the accident until its official end on 16 December 2011 (cold shutdown). The available monitoring data has not been extensively utilized in the present study, in which our scope is limited to general-level comparisons between VALMA and data from other sources.

The task of modelling is made difficult by the fact that the release consists of discharge from several plant units, and possibly the spent fuel pools. The simulation results may be sensitive to some pieces of data in the source term input and weather data. The only variations of source term that were allowed by the project resources were calculations with progressively more complex definition in terms of duration, nuclide content and temporal behaviour. These variations did not reveal abrupt changes in the calculated results, indicating that a simple source could be used as an approximation.

To make the comparison of the material presented above easier, the numbers of VALMA result images are listed in Table 9 along with the corresponding reference publications and the figure numbers in Chapter 4.2.

Table 9. Comparison table of the simulation and monitoring results.

| VALMA result | Monitoring result | Nuclide and date | Monitoring location / region | Reference for monitoring results |
|-------------------|-------------------|-------------------|-------------------------------|----------------------------------|
| Concentrations | | | | |
| Figure 27 (left) | Figure 16 | I-131 / March 12 | Fukushima region | Nagai et al. (2012) |
| Figure 27 (right) | | I-131 / March 13 | | |
| Figure 28 (left) | | I-131 / March 15 | | |
| Figure 28 (right) | Figure 10 | I-131 / March 16 | Tokai-mura | Chino et al. (2011) |
| Figure 29 (left) | | | | |
| Figure 29 (right) | - | I-131 / March 20 | - | - |
| Figure 30 | Figure 8 | Cs-137 / March 15 | Tokai-mura | Stohl et al. (2012) |
| Depositions | | | | |
| Figure 31 (left) | Figure 18 | Cs-137 / March 13 | Northern Honshu | Nagai et al. (2012) |
| Figure 31 (right) | | Cs-137 / March 16 | | |
| Figure 32 | | Cs-137 / March 20 | | |
| Dose rates | | | | |
| Figure 33 (left) | Figure 19 | March 15 | Fukushima-Ibaraki prefectures | Nagai et al. (2012) |
| Figure 33 (right) | | March 16 | | |
| Figure 34 (left) | | March 16 | | |
| Figure 34 (right) | | March 12 – 20 | | |

8.1 Concentrations

It is seen that on March 12 at 09:00 UTC, near the beginning of the release, the monitoring data (Nagai et al. 2012) presents a concentration of I-131 of 37 Bq/m³ (inland north of the NPP site, 37.5 N) whereas VALMA has predicted almost ten times higher levels. On the same day 12:00 UTC, the monitoring data presents concentrations of I-131 of 63-165 Bq/m³, while VALMA has predicted approximately 300 Bq/m³ and the VALMA cloud is more on the coast.

On March 13 at 18:00 UTC, inland west of the NPP site, the monitoring data presents a concentration of I-131 of 60 Bq/m³, whereas VALMA has predicted values ranging from 100 to 1000 Bq/m³ but the VALMA cloud is on the other side of the site. However, there is no concentration measurement from the area of the VALMA cloud.

On March 15 at 01:00 UTC in Tokai-Mura (approximate location 36.5 N, 140.5 E), the monitoring data (Chino et al. 2011) presents observations of 100 Bq/m³, whereas VALMA has predicted as much as 3000 Bq/m³. However, there could be a problem related to the cloud timing (due to insufficient weather data) as just some 2 or 3 h earlier Chino's observations also reach even 2800 Bq/m³. On March 16 at 00:00 UTC, the monitoring data in Tokai-mura presents observations of 300 Bq/m³ whereas VALMA has predicted only 100 Bq/m³. For the end of the examined period on March 20, no exact comparison data was available.

On March 15 at 00:00 UTC, the monitoring data for Cs-137 concentration presents observations of 10 - 200 Bq/m³ in Tokai-mura, whereas VALMA has predicted approximately 300 Bq/m³.

8.2 Depositions

For March 12, the monitoring data presents an area of dry deposition of Cs-137 to the north of the NPP site with values approximately 60 kBq/m². VALMA predicts for March 13, 0:00 UTC, values in the same area ranging from 10 to 50 kBq/m². On March 15, the monitoring data shows areas of dry and wet deposition, side by side, of Cs-137 to the southwest of the NPP site with wide-area highs below 100 kBq/m². The VALMA deposition-affected area is more west-dominated and has values generally somewhat more than 100 kBq/m² (on March 16 at 00:00 UTC).

For March 20, the monitoring data presents an area of wet deposition of Cs-137 to the north of the NPP site with values approximately 10 kBq/m². In comparison with March 16 data, VALMA has predicted a new deposition-affected area to the north-west of the NPP site but much closer to it (on March 20 at 12:00 UTC). VALMA values of Cs-137 deposition in that area are generally more than 100 kBq/m². The non-matching location could be explained by the use of one-point weather data. In any case, the cloud has probably travelled and dispersed less leading to higher deposition.

In general, the caesium ground deposition is highest in the areas northwest from Fukushima Dai-ichi according to measurements and simulations. The maximum Cs-137 deposition on March 20 according to VALMA is the order of 1000 kBq/m². According to the measurements by MEXT (2011), the deposition in the areas with highest contamination is 3000 – 30 000 kBq/m² for both Cs-134 and Cs-137 and 3000 – 14 700 kBq/m² for Cs-137 (as of April 29, 2011). The map by Nagai et al. (2012) suggests depositions of 1000 kBq/m² - 3000 kBq/m² northwest of the site. High deposition is predicted by VALMA also into the ocean south and southeast from the plant site but no measurements are available outside the mainland of Japan (in the references of the study). Somewhat similar values of total Cs-137 deposition in the ocean area have been obtained with simulations by Stohl et al. (2012) (Figure 35).

8.3 Dose rates

The monitoring data for dose rates by Nagai et al. (2012) present measurements of 2.54 and 19.96 $\mu\text{Gy/h}$ to the south-west of the NPP site, together with SPEEDI-MP simulations. For the same area, VALMA values are generally more than 10 $\mu\text{Gy/h}$, ranging up to 100 $\mu\text{Gy/h}$ on March 15 at 00:00 UTC simulation time. For the simulation result at March 16 03:00 UTC, there is currently no comparison data. On March 16 at 12:00 UTC, the monitoring data presents high values (3.49 to 25.06 $\mu\text{Gy/h}$) to the northwest from the NPP site, together with SPEEDI-MP simulations. For the same time and area, VALMA-predicted dose rates generally exceed 50 $\mu\text{Gy/h}$, ranging up to hundreds.

The monitoring data found in the reference literature is rather scarce but, generally, the VALMA prediction seems to be greater than the measured values mapped by Nagai et al. (2012), at most about 100 $\mu\text{Gy/h}$ in Figure 19. In the NPP site, ROSA predicts a maximum dose rate as high as 150 mSv/h at 200 m distance, with a decrease to 2.9 mSv/h at 10 km distance. This result is poorly comparable to the VALMA and monitoring results due to different input assumptions and monitoring points.

For the badly affected village of Iitate, the monitoring data presents a temporal trend of dose rate with rise between March 15, 02:00 UTC and March 15, 09:00 UTC from zero to 50 $\mu\text{Gy/h}$. The corresponding VALMA temporal trend for Iitate (approximate location 37.4 N, 140.6 E) rises to 75 $\mu\text{Gy/h}$ quite steeply on March 15, 08:00 UTC.

8.4 Suggestions for future work

The work could be continued on three fronts: 1) Continued literature survey to find new public data of the estimated radioactive releases and measurements in the environment, 2) extensive calculations with VALMA using all the site-specific weather data and several source term assumptions, and comparison of the deposition and external dose rate predictions with measurements and 3) Code-to-code comparison of VALMA with at least one of the following computer codes: ROSA (by VTT), or the NRC codes MACCS, RADTRAD or RASCAL. It is emphasized here that the current one-point weather data may only be considered adequate for validation of the codes within short range, approximately 20 km, of the source point. So if resources permit, acquisition of other weather data points near the damaged plant (e.g. 6 more points at the distance of 15 km) will be considered. For reliable validation over a wider area, the SILAM dispersion model operated by FMI could be used. Particle trajectories calculated by SILAM can be used for dose assessment with source term variations in VALMA.

More specifically, the suggested improvements to the modelling approach include

- Creating several complex source term assumptions according to literature or VTT MELCOR simulations, running simulations with them and even perform an automatic comparison with measured data available in numerical form, in order to find out which source term assumptions seems most plausible.
- The height distribution of source could be covered better by having more trajectory starting heights than only 20 m and 100 m.
- VALMA could directly utilize mixing heights and washout coefficients from a SILAM run; in this study, mixing heights were set according to stability class, and washout coefficients were calculated from rain intensity in SILAM-like fashion but possibly not as accurately.
- VALMA offers the user to define a set of “probe locations” for which the trends of all quantities are directly produced. With some additional work, such probes could be set

according to where measured temporal trends of concentrations or dose rates were published.

- For better understanding of nuclide-wise released activities, the figures from several estimates should be tabulated side by side, with the nuclides grouped according to their common behaviour, using e.g. the classification by Sevon (2012), and comparing the figures with original inventories of the reactor cores and spent fuel pools.
- With more working time, the time-height distributions of source in VALMA input could be made more accurate by defining them for more nuclide groups separately and by increasing their temporal and vertical resolutions.
- With minor source code modifications and compiling, the Windows based GUI could be made to accept more than 200 time steps. Now this was a restriction that led to calculating at 1 hour steps up to 199 hours from release start. It must be emphasized that this was only a GUI restriction (in visualization); the calculation part can accept as many time steps as memory permits. However, the restriction leads to some artificial “zebra striping” of the radioactive cloud.
- The trajectory calculation subroutine of VALMA would benefit from a slight modification to better cover the whole starting height interval of the release.
- For more detailed, point-to-point comparisons of the monitoring and simulation results could be made by utilizing the Fukushima monitoring database provided by IAEA (<https://iec.iaea.org/fmd/>)

9. Conclusions

A literature search was done to collect background material on source term estimates (including nuclide-specific released activities, temporal evolution and height distribution), measured fallout, concentration in air and external dose rates, as well as atmospheric dispersion simulations by some foreign codes. Samples of this background material are included in this report. Some scoping calculations of dose rates were done with the ARANO-based ROSA code. VALMA inputs were prepared for a hypothetical weather mast at NPP site for several source distribution assumptions, and for generating simulated results for available measurement points. The weather mast data is actually interpolated from the ECMWF NWP model, with the interpolation performed by FMI. VALMA results are available both on a map background (some 250 x 250 km around site) and as temporal trends at chosen geographical points. Overall comparison of measurements and simulations were made.

As in all assessments of dispersion of accidental atmospheric radioactive releases, the two main sources of uncertainty are the source term and the weather data used. Considering the Fukushima accident, new estimates of releases continue to be published as information and understanding of the progression of the accident is accumulated. However, it must be emphasized that it is not enough to know the total released activities of the nuclides (about which there are even wildly differing figures in some cases). As weather conditions continually change as a function of time and location, it is also essential to know their temporal and vertical distributions. In the vertical, release height is affected by heat content of the emissions and by possible explosions etc. Concerning weather data, data based on a numerical weather prediction model (NWP) is usually considered best, as it is available as time-dependent 3D fields and has been produced by CFD which accounts for mass continuity, among other things. Only in the immediate vicinity of the NPP can we say that measured weather data may be better. In this study, the weather data is a great source of

uncertainty. Though originating from the ECMWF model, it was generated for simpler codes than VALMA. For that reason, it only simulates a measurement point at Fukushima Dai-ichi NPP.

For these reasons, the present short study should not be considered as a validation of VALMA. Neither can it directly be used to find flaws in the VALMA simulations. For example, the “zebra striping” in VALMA results is not an artefact of VALMA algorithms as such, but due to using too long time steps (for practical reasons). First and foremost, this study is a quick scoping study, where one can by comparison with published measurements see if the corresponding simulated quantities have at least approximately the right timing, location and magnitude. It also served as an interesting test case for VALMA’s mast based prediction capability which has not been used as much as the better SILAM based one.

References

- Chino, M., Nakayama, H., Nagai, H., Terada, H., Katata, G., Yamazawa, H. 2011. Preliminary estimation of release amounts of I-131 and Cs-137 accidentally discharged from the Fukushima Dai-ichi NPP into the atmosphere. *Journal of Nuclear Science and Technology*, vol. 48, No 7, p. 1129-1134.
- Ducros G, Pontillon, Y., Eschbach, R., Vidal, J.M., Le Petit, G., Douysset, G., Poinssot, C. 2012. Main lessons learnt from fission product release analysis, for the understanding of Fukushima Dai-ichi NPP status, *Severe Accident Assessment and Management*, San Diego, California, November 11-15, 2012.
- Hirose, K. 2012. 2011 Fukushima Dai-ichi nuclear power plant accident: summary of regional radioactive deposition monitoring results. *Journal of Environmental Radioactivity* 111, p. 13-17.
- Hosoda, M., Tokonami, S., Sorimachi, A., Monzen, S., Osanai, M., Yamada, M., Kashiwakura, I., Akiba, S. 2011. The time variation of dose rate artificially increased by the Fukushima nuclear crisis. *Scientific Reports* 1 : 87, DOI: 10.1038/srep00087
- IAEA. 2012. Fukushima Monitoring Database. <https://iec.iaea.org/fmd/default.aspx>. Referred on February 19, 2013.
- Ilvonen, M. 2002. Constrained optimization of the VALMA dose assessment model by a genetic algorithm, Lic.Sc. (Tech.) Thesis, Helsinki University of Technology.
- Ministry of Education, Culture, Sports, Science and Technology and the U.S. Department of Energy. 2011. Results of Airborne Monitoring, May 6, 2011 (http://www.mext.go.jp/component/english/_icsFiles/afieldfile/2011/05/10/1304797_0506.pdf referred on February 19, 2013)
- Ministry of Education, Culture, Sports, Science & Technology in Japan (MEXT), <http://www.mext.go.jp/english/>, referred on February 19, 2013.
- Nagai, H., Chino, M., Terada, H., Katata, G., Nakayama, H., Ota, M. 2012. Source term estimation and atmospheric dispersion simulations of radioactive materials discharged from the Fukushima Daiichi Nuclear Power Plant due to Accident. Presentation at JAEA SPEEDI-MP International Workshop, February 22-23, 2012.
- Sevon, T. 2012. Status Report of MELCOR Modeling of Fukushima Daiichi 1 Accident. VTT Research Report, VTT-R-00215-13, Espoo, Finland. 40 p.

Stohl, A., Seibert, P., Wotawa, G., Arnold, D., Burkhardt, J. F., Eckhardt, S., Tapia, C., Vargas, A., Yasunari, T.J. 2012. Xenon-133 and caesium-137 releases into the atmosphere from the Fukushima Dai-ichi nuclear power plant: determination of the source term, atmospheric dispersion and deposition. *Atmos. Chem. Phys.* 12, p. 2313-2343.